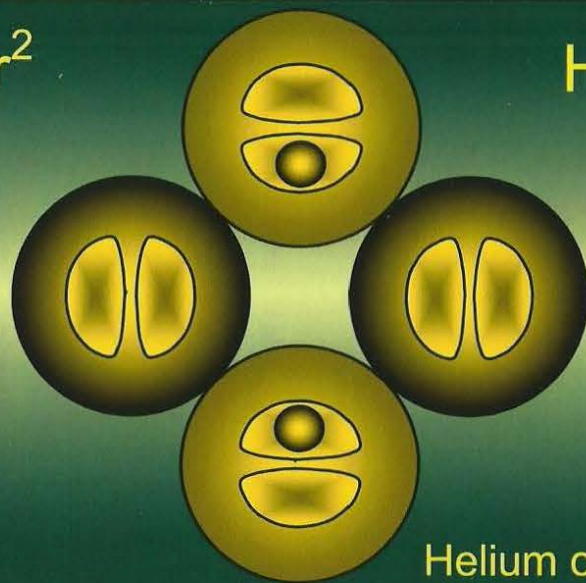# Konstantin Meyl

From **Nuclear Physics** and **Fusion** to **Nanotechnology**

From **Nuclear Physics** and **Fusion** to **Nanotechnology**

by **Prof. Dr. Konstantin Meyl**

$E \sim 1/r^2$ $H \sim 1/r^2$

Helium core

Coulomb's law stating that the electric field decreases proportionally to the square of the distance ($E \sim 1/r^2$) is equal in meaning to a length contraction dependent on the field. Based on this, the mass defect of an atomic nucleus is determined mathematically accurately.

Furthermore, the model of potential vortices yields accurate values for the diameters and shapes of nuclei, which are always compared to the known quantum properties. The riddle of the halo nuclei is solved on the way. The strong interaction is simply a magnetic attraction of the nucleons. The atomic shell kept together by the electric field forces is calculated afterwards. Even this is based upon the dependency of the radius values on the field. An equation is derived with which the atomic radii of all known elements and partially even their ions may be calculated. The correlation to known measurement values was successful, across the domain from Helium to farther than plutonium, with a precision never seen before, which gives reason for the validity of the model.

Thoughts on monatomic structure as a prerequisite for the application of cold fusion and nanotechnology constitute the end of the book.

Derivation and calculation of atomic nuclei, periodic table of elements, and monoatomic elements at nano scale, based on recently discovered potential vortices

Derivation and calculation of atomic nuclei, periodic table of elements, and monoatomic elements at nano scale, based on recently discovered Potential vortices

4

From **nuclear physics** and **fusion** to **nanotechnology**
from the series **Potential Vortex,** Volume **4**

Professor Dr.-Ing. Konstantin Meyl

1st Edition (2012), with 39 pictures and 114 pages

Preface

"That can't have been it", I thought to myself 20 years ago after successfully validating my extended field theory by deriving from it both the Schrödinger equation and the quantum properties of elementary particles.

If the potential vortex theory aims to be a "theory of everything", it must allow for the behavior of all known subatomic particles to be derived from it mathematically. There is an abundance of experimental data to validate the calculated results against, and we're only able to claim knowledge about the interrelations once we have been able to successfully calculate them.

There was plenty of incentive. Thus, I began creating spherical vortex diagrams of the nearly 100 known nuclei in 1995. But then, about half way through, I gave up. Having allowed for too many degrees of freedom, I had become mired in ambiguities.

I found solace in the fact that all hitherto existing models of nuclear physics were themselves not borne out of a singular unified one. Therefore I concluded that it should be sufficient to publish my approach in volume [2], wait a while and let other scientists take up my model and refine it accordingly in the meantime.

And so I waited and nothing happened – almost nothing, at least for a decade. Only then did a colleague mentioned in volume [3], Kaiser (pseudonym) [4] realize the potential of my field theory and begin with the respective work. Unfortunately, his efforts also ended in ambiguities not suited for proof.

However, the intersection of the rules for the potential structures of nuclei compiled by both of us eventually yielded success, as documented in this book.

By now, my colleague is retired and I'm enjoying the tranquility of a sabbatical term. Meanwhile, I've come to believe that it's necessary to rely only on myself, considering the stagnant state of theoretical nuclear physics and its persistent lack of progress.

Having finishined the revision of the existing volumes from the potential vortex series and having begun my jounrey into nuclear physics, confirmations and insights are literally pouring in, which is surprising even to me. Rather than delving into established textbook science, I will discuss experimental results that are generally considered mysterious or incalculable in this book.

Here's hope that it won't take another decade for the potential vortex theory to gain recognition in scientific circles and that many "hunters and gatherers" in the form of research groups take up these ideas and become inspired by them. Only collectively can the great challenge of unifying the concurrent patchwork physics be accomplished.

Konstantin Meyl   www.meyl.eu

Villingen-Schwenningen, February 2012

Table of Content   Page

1. Overview

The mass defect of nuclei interpreted as bonding energy has been measured with precision, yet remains neither explained nor calculated. Both shall be made good for in the following pages.

All known quantum properties of protons and neutrons, the building blocks of nuclei, are described without constraints by a field vortex model. The mass of the nucleons can be calculated by the internal structure, the mass defect by the distribution of charges within the respective vortex structures.

The derivations from the novel nuclear model put the stability of alpha particles, nuclear fission and fusion energy in a whole different light.

1.1 The trivial "abnormal" spin-g-factor of the electron

The very extensive foundations of the following treatise fill the first three volumes of this series on potential vortexes.

Volume [1] revolves around vortex physics contrasted with quantum physics [1]. The derivation of the Schrödinger equation from laws of field physics suggests that atoms are structured as electromagnetic field vortexes. The pressure resulting from the contracting potential vortex and acting from all sides causes the spherical structure.

The model of an elementary vortex depicted in fig. 1.1, which perfectly covers all properties of an electron, was created in this way.
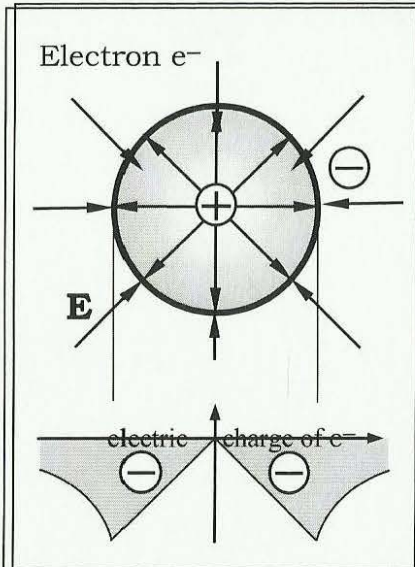
Fig. 1.1:   *The electron as a potential vortex configuration*

It is an electric monopole if the expanding vortex on its inside (with its characteristic time constant τ_1) and the outside contracting vortex (with τ_2) acting in opposition to it are of equal magnitude ($\tau_1 = \tau_2$). This is confirmed by calculation [Volume [1], Eq. 8.13].

Observed from the negatively charged vortex perimeter, the positive counterpole is situated within the vortex core, which is why the vortex model of the electron describes an electric dipole, one pole of which is hidden invisibly and immeasurably on the inside. However, a glance upon the charge distribution reveals a zero charge, provided that the vortex core is in a restful state similar to the infinite.

Thus, the monopole's charge is greater than the dipole's by the known Landé factor $g_e \cong -2$, which places the zero point at the midpoint between the positive and negative poles, as usual. The g_e-factor might be extremely trivial, yet is brought to bear on the magnetic moment:
$$g_e = -2\,|\mu_e/\mu_B| \qquad (1.1^*)$$
with the Bohr magneton:
$$\mu_B = e\hbar/2m_e = 927{,}4 \cdot 10^{-26}\ \text{Am}^2\ . \qquad (1.1)$$

The distance between the measuring apparatus and negative shell of the monopole is also of significance. Ideally, there would be an infinite distance from the monopolar charge. That, however, is a technical impossibility, as the measuring technician has to approach his object of interest somehow. Minor yet still significant errors on the scale of $1^0/_{00}$ are therefore unavoidable.

Furthermore, the second volume addresses the question of why the spherical structure is not in contradiction to the requirement of perpendicularity of the electric field **E**, the magnetic flux density **B** and the vortex rotation **v** [2, Eq. 2.1]:
$$\mathbf{E} = \mathbf{v} \times \mathbf{B}. \qquad (1.2)$$

The answer is determined mathematically by deriving a field expansion from the Lorentz contraction [2, Eq. 2.20]:
$$E \sim 1/r^2\ . \qquad (1.3)$$

1.2 The rotating spherical elementary vortex

On the inside of the spherical vortex, where all field vectors are pointing towards the vortex core, causing (for $r \to 0$) not only the dimensions (in [m]) but also the vortex velocity v [m/s] to approach zero, a singularity reminiscent of a miniature black hole is found. But only once the velocity reaches zero does the field vortex exhibit the Cartesian firmness common for matter.

Outside of the particle, the open electric field lines cause the electromagnetic interaction, while the closed magnetic field lines cause an attractive force according to eq. 1.3. that we refer to as gravitation.

If we reverse all vectors in fig. 1.1, the image depicts the properties of a positron, or more generally speaking: As there are always two diametrically opposed modes of vortex rotation, there exists a complementary antimatter particle to every matter particle. Thus, the inside of an electron contains a positron and vice versa.

The field necessary to maintain the spherical structure is generated autonomously by each field vortex through its self rotation according to eq. 1.2. It is for this reason that the vortex velocity is determined and the particle exhibits a quantized spin of

$$s = \pm \tfrac{1}{2} \ . \tag{1.4}$$

As a vortex particle with both electric charge and angular momentum, it possesses a dipole moment that can be influenced by magnetic fields (Zeeman effect). On account of the aforementioned g-factor, the doubled orbital angular momentum causes the electron to exhibit an equally doubled magnetic moment.

1.3 Protons without nuclear energy

Volume [3] on potential vortexes delves into the known tendency of electrons to form pairs. Electrically, the similarly charged particles are repulsive, but given an antiparallel orientation of their spin axes, they are attracted magnetically. According to calculation, the magnetic attraction exceeds the electric repulsion ([3], Eq.4.10) and therefore makes the postulated structure appear plausible.

In the realm of antimatter, two positrons will form a doubly positively charged pair. It strongly attracts negatively charged electrons.
Under lab conditions, annihilation gamma radiation would be observed, which could theoretically be avoided if the electron absorbed the positron pair. This should occur smoothly, considering the field configuration of a positron as well as its vortex rotation should be manifest within an electron's interior.

The proton p+:

mass $m_p = 1836 \, m_e$ (measured)

charge $Q = +1+1-1 = +1$

spin $s = \tfrac{1}{2}$ (predetermined by exterior elementary vortex)

Landé-factor $g_p = 2(\mu_p/\mu_N) = 5,59$

magnetic moment $\mu_p/\mu_N = 2,79$
pointing in the same direction for all 3 vortexes.

Fig. 1.2   *The interior structure of a proton*
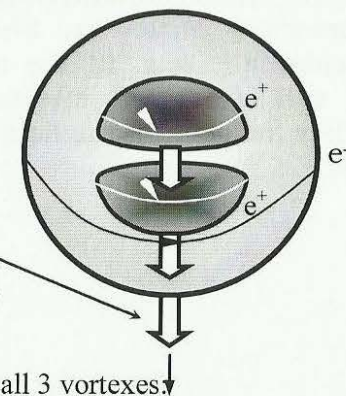
The unit consisting of 3 vortexes is represented in fig. 1.2 (see also [3], fig. 5.2). With its spin of the external electron, its almost threefold magnetic moment and its singular positive charge, it is obviously a proton.

Only on the surface of the proton can the negatively charged electron vortex compensate punctually for the field generated by the pair of absorbed positrons, which is why there is no charge that could cause attractive or repulsive forces.

The calculated field pattern, itself mostly congruent with the measurements, can thus explain the cohesion of the similarly charged protons in a nucleus, wholly without invoking a strong nuclear force or a fictitious potential well.

Nonetheless, a diproton can not exist, as a convergence is only permissible in case of counter-rotation with identical circumferential velocity. There is no location, however, that would allow for contact between two protons while maintaining attraction due to their symmetrical structure. Should two protons coalesce coincidentally (e.g. in the nucleus of an H_2-molecule), they will either not interact at all or even repel one another (respecting the field pattern of a p+, vol. [3], fig. 5.3 and 5.4).

1.4 The asymmetry of neutrons

Contrary to protons, neutrons display an inner charge distribution. This is confirmed both by measurements as well as calculations in volume [3]. In terms of vortex theory, the question is where to find an additional electron vortex within the proton. This is only allowed for one of the two positrons, for only there the respective vortex orientation can be present.
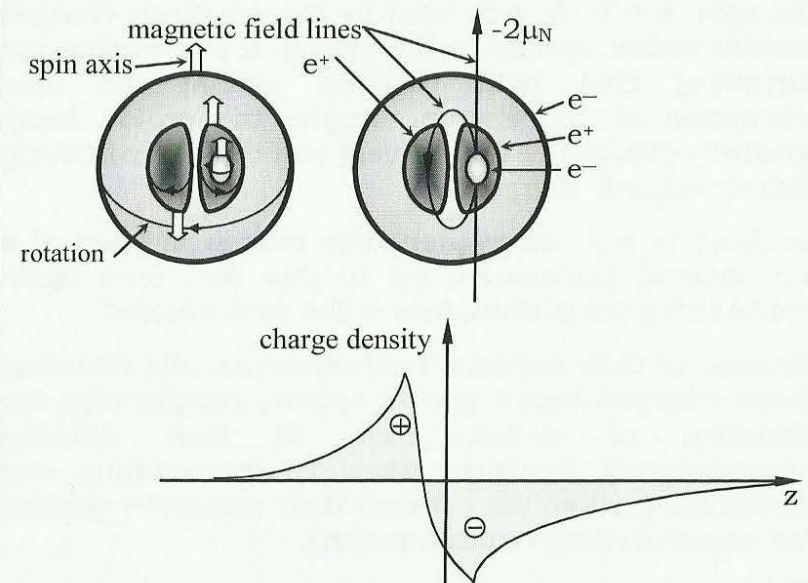
Fig. 1.3: *The neutron and its calculated charge density distribution charge:* $Q_{average} = 0$,   *spin:* s = ½ *(like e⁻)*
magnetic moment: $\mu_n = -1,913 \cdot \mu_N$
mass: $m_n = 1838,7 \cdot m_e$, $g_n = 2 \cdot \mu_n / \mu_N = -3,83$

Fig. 1.3 depicts the magnetic dipole moment of the contained electron and shows how the field line closes above that of a positron still within the neutron. What remains are the magnetic fields of the second positron and the enveloping electron.

In practise, the theoretical value of the magnetic moment $2 \cdot \mu_N$ is thus reduced to

$$\mu_n = 1,913 \cdot \mu_N \qquad (1.5)$$

because, as with all dipoles, stray fields emerge, the internal proportion of which are impossible to measure.

The spin $s = \frac{1}{2}$ is generated by the negatively charged exterior vortex, similar to the proton. It is therefore not surprising that both particles exhibit the spin orientation of an electron, despite the proton being positively charged in the far field and the neutron being entirely without charge.

Needless to say, those properties remain in want of a conventional explanation up to this day, once again emphasizing the performance of the vortex model.

Because of their asymmetrical structure, the neutrons shape diverges from a perfect sphere, complicating the formation of n^o-pairs due to their differing circumferential velocities when counter-rotating and experiencing attraction between their respective positive and negative charge concentrations.

Within large nuclei, the lacking symmetry is obviously being induced in order to allow for frictionless rotation of the nucleons.

2. Calculated mass defect

Now that the models for nucleons are on the table, the real work can begin. It is reminiscent of a huge puzzle, the pieces of which are protons and neutrons supposed to ultimately form a picture of the Karlsruhe nuclide chart, which remains full of mysteries up until today.

In addition, the puzzle pieces are shrinking and losing mass when put together, which has driven many players into desperation. How is the whole supposed to fit together and how is the resulting picture supposed to look?

The current state of physics assumes a closed system, leaving the number of nucleous unchanged. In this scenario, the mass defect Δm according to the Einstein-formula is

$$\Delta E = \Delta m \cdot c^2 \qquad (2.1)$$

converted into an energy differential ΔE which is interpreted as bonding energy. Through fission of heavy nuclei in nuclear plants this released energy is harvested.
It is still a mystery what kind of bonding force keeps nuclei together and which physical mechanism is responsible for the changes in nucleon mass.

It is clear that the mass defect falsifies the postulate of classical physics according to which all matter is conserved at all times (Lomonossow (1748) – Lavoisier (1789) – law). Only an exact calculation of the particle mass (see vol. [3]) will shed light on these unresolved questions.

2.1 Deuteron

The hydrogen nucleus consists of only a single proton, which is why no mass defect can be observed.

Things become interesting only once a nucleus is made up of two or more nucleons.

We begin with deuterium, also known a heavy hydrogen. Its nucleus (deuteron $_1^2H$) consists of one proton and one neutron. The spin of both nucleons should add up to s = 1, while the magnetic moment during reciprocal magnetic attraction should be reduced to approximately: $\mu_p - \mu_n \cong 3\,\mu_N - 2\,\mu_N = \mu_N$
(measured value minus stray fields: $\mu_d = 0{,}86\,\mu_N$)   (2.2)

The singular positive charge of deuteron is contributed by the proton. Measurements yield a mass defect of 0.118 % .

What does the vortex model predict? The nuclear physicist Kaiser [4] discusses three different convergence cases of protons and neutrons according to the MFT (Meyl field theory).

Fig. 2.1: *Couplings of protons and neutrons in deuteron*
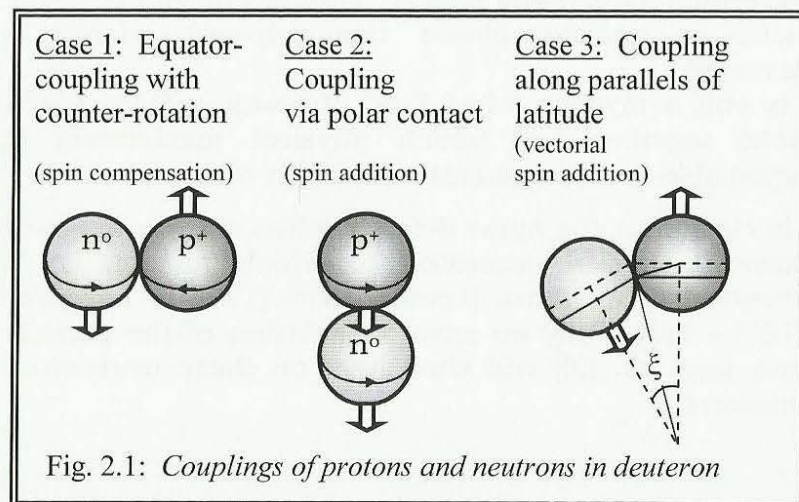
He favors the second case of a coupling along the poles, yielding a spin of s = 1. In my opinion, the deuteron is also capable of attaining a zero spin, as the magnetic moment definitely supports the first case. Possibly, the magnetic field emitted by the measuring apparatus is able to rotate the structure. Another argument in support of the first case is the electric attraction between the neutron's negative charge concentration and the proton's positive charge distribution, which is only provided in case of counter-rotation.

Due to the asymmetric structure of the neutron, deviation from a perfect sphere is expected, meaning different radii, similar to a potato, allow the proton to only approach the neutron where the circumferential velocities of both rotating bodies are equal. This lends credence to special case number three.

Consequent to their differing radii, proton and neutron will rotate around one another along their shared center of gravity lines. Therefore, the nucleus' angular momentum vector will display precession relative to the orientation of the atomic shell's magnetic field.

Both the arising centrifugal force as well as the electric and magnetic attractions lead to slight deformations of the vortex structures. This causes said mass defect. In case of the deutron, it is very minor due to the many degrees of freedom provided by only two counter-rotating nucleons.

If more nucleons are added,, the degrees of freedoms are reduced   and the emergence of structures initially increasing the mass defect is induced forcefully. A mathematical explanation for this is still to be found.

2.2 The new - old Pauli Exclusion Principle

Next, we want to add another nucleon to the deuterium nucleus. In case of equatorial coupling, the "Pauli Exclusion Principle" takes over.

The triplet configuration would be akin to a gearbox in which any two of the triangularly arranged gearwheels block one another.

One could also interpret the exclusion principle as a rule that there may not be triangular spaces in between nucleons [4].

Fig 2.2: *The recommended symbol for the Pauli Exclusion Principle [4].*

Only a configuration incorporating respectable distances or one where all three nucleons form a line is allowed, as long as their rotation occurs in perfect synchronicity.

Fig. 2.3: Triton $_1^3$H.

$\xi =$	0°	60°	90°
$s =$	+½	+½	+½
$\mu_t/\mu_N =$	−1	+1	+3

$g_t = 2\mu_t/\mu_N$, $Q = 1$ e
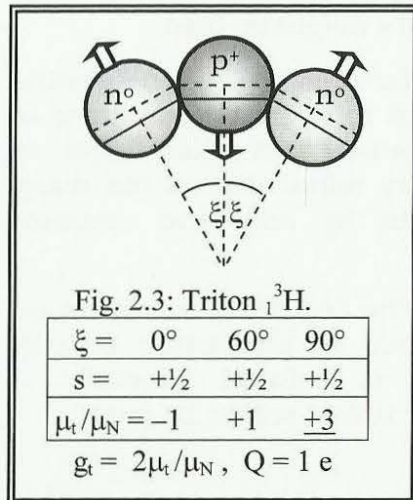
Thus, a tritium nucleus $_1^3$H has two neutrons sandwiching one proton. As they repel one another due to their similar spin orientation and only experience attraction by the proton, they will remain on opposite positions in case of rotation. This holds true for rotations along a latitude below $\xi = 90°$.
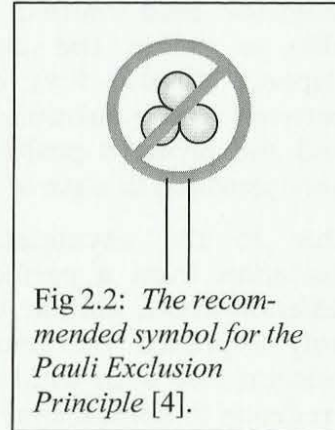
This constellation seems very likely in regards to spin and the magnetic moment.

The cause for the more than doubled mass defect is mostly the proton, which is being deformed from two sides simultaneously.

The triton is not very stable and decays with a half life of 12.3 years via β⁻-decay into a helion, the nucleus of the stable helim isotope $_2^3$He:

$$_1^3H \rightarrow {_2^3}He + e^- \qquad (2.3)$$
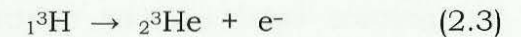
Possibly stimulated by a neutrino, neutrons within the tritium nucleus "spit out" their absorbed electron and thus transmute into a proton. Presumably, it then moves to the other side along its polar coupling and thus performs a flying spin change.

The stable end result is again made up of three nucleons. However, this time two protons sandwich one neutron. The spin remains s = ½ .

These explanations about triton $_1^3$H, includingg degrees of freedom, structure, angular momentum and the gyromagnetic momentum, equally apply to helion $_2^3$He. Fig. 2.4 briefly summarizes the predictions:

Fig. 2.4: Helion $_2^3$He consisting of:
spin   s = ½
charge   Q = 2
and $g_h = 2\mu_h/\mu_N = -4,26$ Landé-factor, with the
magnetic moment:: $\mu_h/\mu_N \cong -2 (...-4)$ bei $\xi \leq 90°$
in this case: $\mu_h/\mu_N = -2,13$ bei ca. $\xi = 59°$
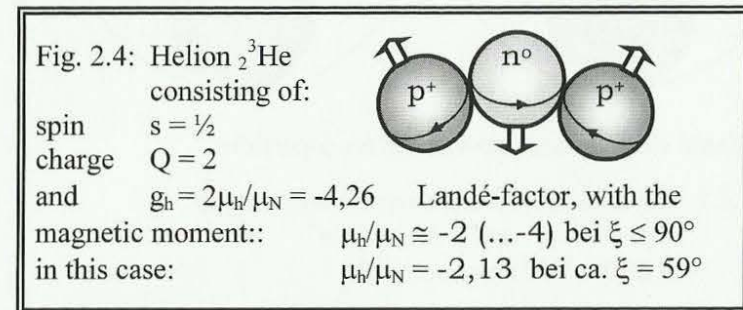
2.3 The properties of α-particles

Two protons and two neutrons form a nearly perfect nuclear structure. It is known as the helium nucleus $_2^4$He or α-particle.

In its case, the electromagnetic attraction between protons and neutrons, as already discussed for deuteron $_1^2$H, is manifested four-fold. The structure of triton $_1^3$H, in which two neutrons sandwich one proton, just like two protons sandwich one neutron in case of helion $_2^3$He, now exists twice, respectively.

According to the vortex model, this accumulation of bonding principles provides the α-nucleus with its well known high stability.
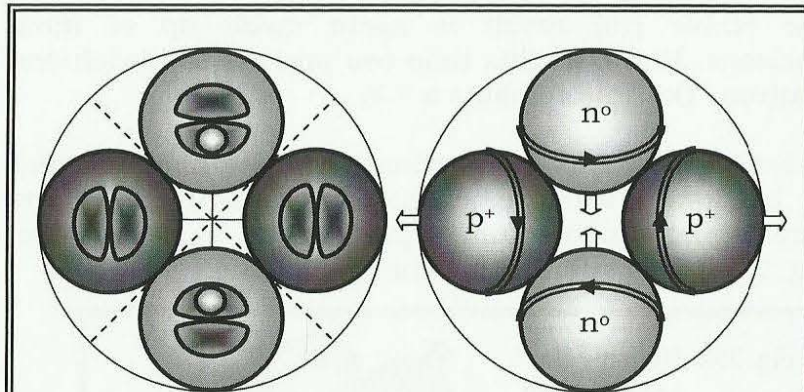
Sectional diagram and top view of an α-particle

Fig. 2.5: *the structure of α-particles consisting of 2 protons p$^+$ and 2 neutrons n^o with ξ = 90° rotation angle.*

In the constellation depicted in Fig. 2.5, the nucleons unroll along latitudes below the threshold angle of ξ = 90°. In case of total spin compensation (s = 0), the magnetic moment vanishes entirely, as every neutron is connected to every neighboring proton by field lines proportional to the nuclear moment μ_N minus the stray fields.

But as the proton possesses 3 such field line clusters, one remains left over. In the displayed configuration, one proton's residual field moves over to the left, the other's to the right. This way, the basis of a magnetic monopole is formed.

If the α-particle is exposed to an external magnetic field, it enters a defensive posture, trying to counteract the disturbance. This is called diamagnetism (rel. permeability $\mu_r < 1$)
which determines the magnetic susceptibility of the α-particle to be

$$\chi_m = \mu_r - 1 = -1.1 \cdot 10^{-9} \qquad (2.4).$$

According to the vortex model, the nucleus reacts by unrolling at a slope angle of ξ. It reacts diamagnetically by altering its latitude.

2.4 The properties of helium nuclei

If we consider the other extreme of ξ becoming 0° by unrolling of the nucleons along their respective equators, the spin compensation (s = 0) as well as the two-fold positive charge remain. The magnetic moment however increases from from 0 to $2 \times \mu_N$ (Fig. 2.6).

In this constellation, the inert α-particle becomes a reactive nuclear particle exerting magnetic attraction on

other nuclear particles. This guarantees the cohesion of nuclei, as long as the attraction exceeds the nuclear repulsive forces. In this manner, helium nuclei $_2^4$He can be stacked upon one another under the permissible polar arrangements of the respective nucleons of equal rotational direction through magnetic attraction, for example.

Sectional diagram of $_2^4$He-nucleus and   side view

Fig. 2.6: *the structure of helium nucleus $_2^4$He ;(with $\xi = 0°$)*
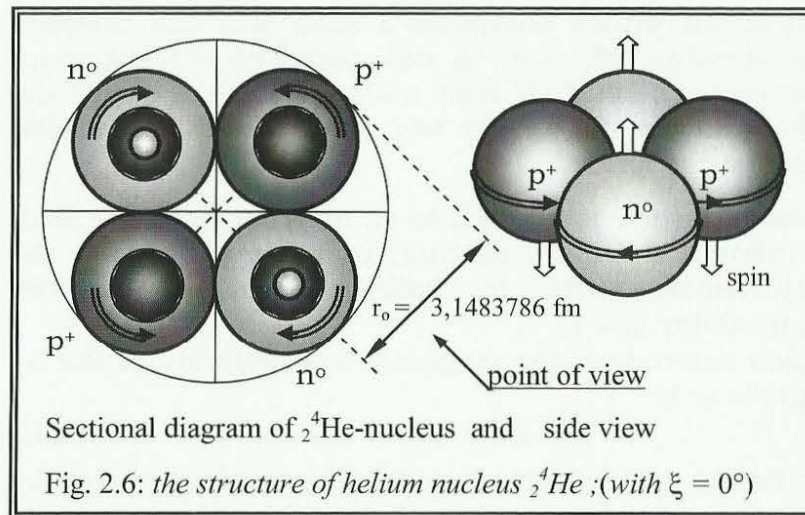
Thus, assuming that large nuclei consist of many of these stacked nucleon-quartets, it appears logical that radioactive decay releases entire α-particles from the cluster. These escaping α-particles, due to their lack of magnetic orientation, will rearrange themselves in open space according to fig. 2.5 and take on a slope angle somewhere between zero and 90° ($0 < \xi < 90°$) without magnetic interaction. Then, the spin indicators displayed in fig. 2.6 (side view) will point obliquely towards the exterior and interior in pairs.

2.5 The inner structure of helium nuclei

To calculate mass and mass defect, we need to understand the inner structure, which is why it is of special interest to us. The occurring inner shifts can no longer be ignored.

To recap [3]: The field energy trapped inside of a vortex particle is equal to the field energy measurable from the outside and acting all the way to infinity. The fields of a vortex within a neutron therefore radiate unobstructedly towards its outside and determine the size and mass of the particle.

However, they also give rise to an electromagnetic interaction, which is responsible for the charge distribution of the neutron, for example. If an attractive force emerges between the negative charge concentration of the neutron's absorbed electron vortex and the proton's positive charge caused by its inner positrons, both will attract one another and shift position within the nucleon.

The inner vortexes converge, reducing the radius of the helium nucleus as measured from the outside by 44%. The dimensions on the inside of the nucleons initially diminish without any effect on mass at the same ratio: $r_1/r_2 = 0.5$.

Their vortex core shifts slightly, however. If we assume the shift totalled only 0,75% of the helium nucleus' radius r_1 in the direction of its center.

It would consequently mean: $r_1 \leq 0.5 \cdot r_2$ or, under the given assumption: $r_1 = 0,498125 \cdot r_2$.   (2.5)

2.6 Calculation of the mass of the helium nucleus

All statements are based on the mass of the electron [5]:
$$m_e = 9,109383 \cdot 10^{-31} \ [kg] \qquad (2.6)$$

If the formerly postulated mass defect was still considered valid, we would only need to add the 4 singular masses of the helium nucleus:

$$m_{He} = 2 \cdot (m_n + m_p)$$
$$m_{He}/m_e = 2 \cdot (1839 + 1836) = 7350 \qquad (2.7)$$

The measured value for the $_2^4$He-nucleus, in contrast, is:

$$m_g/m_e = 7294 \qquad (2.8)$$

which yields a mass loss of $\Delta m/m_e = 56 \qquad (2.9)$
on the magnitude of 0.76 %.

To mathematically verify the measured values, the formula derived in Volume [3] will be used:

$$\frac{m_{He}}{m_e} = 68 \cdot z_e^3 \cdot e_i^2 \qquad (2.10)$$

The 17 most important elementary particles have been successfully calculated in relation to the mass of the electron m_e in this manner (20 years ago already) ([3], Fig. 4.1). z_e denotes the quantity of elementary vortexes involved. e_i denotes the relation of the electric field strength: From the sum of interior field vortexes at the radius of the enveloping electron vortex $E(r_a)$ and normalized to the field strength of an elementary vortex E_1:

$$e_i = E(r_a)/E_1 . \qquad (2.11)$$

(where the subsidence of the field $E(r_a)$ over the radius conditions needs to be considered).

In the case of the proton, we are dealing with 2 positrons. Each generates the field strength E_1 on its surface, subsiding proportionally to the radii $r_1/r_2 = 0.5$ towards the enveloping electron vortex, which is why the field strength $E(r_2) = 2 \cdot E_1 \cdot (r_1/r_2) = +E_1$ occurs there. Thus, $e_i = 1$. The superposition with the electron's field $- E_1$ causes the already mentioned disappearance of the field on the surface of the proton, which therefore qualifies as a nucleon entirely without nuclear forces.

Using three elementary vortexes $z_e = 3$ and the value $e_i = 1$, the formula 2.10 yields the well-known mass of the proton in relation to the electron:

$$\frac{m_p}{m_e} = 68 \cdot 3^3 \cdot 1^2 = 1836 \qquad (2.12)$$

With a radius quotient (2.5) the factor e_i calculates as:

$$e_i = 2 \cdot (r_1/r_2) = 2 \cdot 0,498 = 0,996 \ . \qquad (2.13)$$

while the proton mass theoretically reduces to:

$$\frac{m_p}{m_e} = 68 \cdot z_e^3 \cdot e_i^2 = 68 \cdot 3^3 \cdot 0,996^2 = 1822 \qquad (2.18)$$

and therefore loses about 0.75 % of mass.

As all four nucleons are subject to the same shift in internal structure, the mass defect of the entire helium nucleus is presumably 0.75% (eq. 2.7):

$$\frac{m_{He}}{m_e} = 0,9925 \cdot 7350 = 7295 \qquad , \qquad (2.19)$$

which comes very close to the measured value (= 7294 according to eq. 2.8).

2.7 Summary

This calculation makes it clear that the shift of the positron vortexes inside a proton and towards the center of the helium nucleus by 0.75% also results in a mass defect of a nearly identical magnitude.

This relation, which was identified by coincidence, still holds true for very large nuclei, which can reach mass defects of almost 1%, as is well-known.

Thus, it can be inferred that internal shifts of approximately 1% are caused by attractive electrical forces as well. At this point, a limit is reached that can not be exceeded as the nucleon pairs' counter-rotation may not otherwise be maintained without friction.

The vortex model devised to calculate the quantum properties of elementary particles (in 1992) also performs well in terms of nuclear physics, as it accurately describes the most important quantum properties such as charge, spin and magnetic moment of the various hydrogen and helium nuclei.

In addition, the vortex model is a contribution to a unified theory, as all emerging forces are explained by electromagnetic interaction exclusively.

It is yet to be validated if the postulated rules for small nuclei remain applicable when it comes to medium and large nuclei.

3. The alpha-particle model of vortex cores

The "nucleon puzzle" has not been solved by any means. We still have a large package with over 200 "pieces" ahead of us. Complexity increases accordingly and at some point, the usage of multidimensional math programs becomes necessary, as we are dealing with rotating vortex structures variable in time and space, the building blocks of which revolve around themselves.

Equation 1.2 even allows for the inverse conclusion: that without movement, no fields, no particles and ultimately not even matter could exist at all (see Volume [2]).

But even before utilizing powerful calculating devices, many unresolved questions of nuclear physics can be resolved vividly by consideration. Surely, the vortex model and its derivative equations can be of great assistance in this regard.

There are many competing nuclear models. I am drawn to the alpha-particle model and aim to refine it. According to this model, α–particles form stable sub-units within a nucleus. This provides us with a useful model for integral multiples of the nucleon basis 4, e.g. the nuclei of $_6^{12}C$, $_8^{16}O$, or $_{10}^{20}Ne$. These nuclei are diamagnetic and without spin, and thus of generally similar properties as the helium nucleus.

Cohesion is provided by the magnetic force, calling for helium nuclei (with a rotation angle $\xi = 0°$), which is why the name "alpha-particle model" seems slightly inappropriate. It should be called "helium-vortex-center model", but I will stick with the original name due to the strong similarity to α-particles.

3.1 Exception to the rule (with A=5)

Climbing up the periodic system, we encounter the first deviation from the alpha-particle model when reaching lithium. Still, the isotope's decay signifies its close relationship to the helium nucleus:

$$_3^5Li \rightarrow {}_2^4He + p+ \tag{3.1}$$
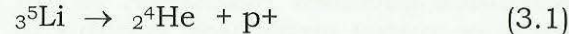
That is to say that upon emitting its superfluous proton, it can attain the highly stable α-state. Let's attempt a three-dimensional depiction (as suggested by [4]), wherein the arrow $\Longrightarrow$ marks the spin axis, a dot the arrow's tip and a cross the arrow's tail. Neutrons are represented by light and protons by dark spheres.

mass number A = 5

decay of the isotopes:

$_3^5Li \rightarrow {}_2^4He + p^+$

$_2^5He \rightarrow {}_2^4He + n^o$

Fig. 3.1: *core structure of the Lithiumisotope $_3^5$Li.*
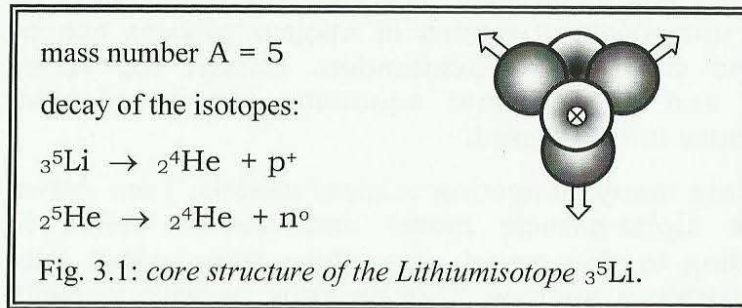
The 4 upper nucleons can indeed be considered an α-particle. The deviation from the model however is that they are in a slanted configuration somewhere in between $\xi = 0°$ and $90°$. Also visible is the forbidden triplet-configuration, calling for respectable distances between the nucleons. To attain stability, further n^o are required.

In case of the helium isotope $_2^5$He, p^+ need merely be replaced by n^o and vice versa. The reason for instability remains the same.

3.2 Lithium nuclei (with A = 6 and 7)

Only the lithium isotope $_3^6Li$ is stable and naturally occurring at a ratio of approximately 7.6%. It might be a combination of a helium nucleus and a deuteron, as the mathematical summation yields the correct values for spin and magnetic moment. As the helium nucleus does not contribute, only the deuteron's values are substantial.

A merging of the nucleons suggests the structure shown here.

mass number A = 6

decay of the isotopes:

$_2^6He \rightarrow {}_3^6Li + e^-$

$_3^6Li$ stabil

$_4^6Be \rightarrow {}_2^4He + 2p^+$

Fig. 3.2: *core structure of Lithium $_3^6$Li.*
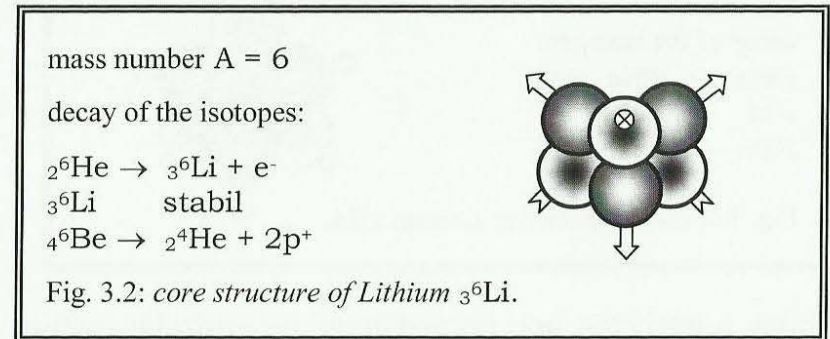
This double triplet configuration might be perfectly symmetric, but demands a large distance in between similar nucleons. As we know, this leads to a significantly reduced mass defect compared to the α-particle.

The particle is without doubt a worthy representative of the alpha-particle model, even though the discernible structures appear at an angle somewhere in between that of a pure α-particle and that of a helium nucleus ($0 < \xi < 90°$).

And so, the spin pointers are spread out in all directions, just like the spikes of a hedgehog, which might grant this nuclear model the name "hedgehog-model" [4].

If we now add another neutron on top, counter-rotating relative to the two protons, we arrive at the common structure of lithium $_3^7Li$. The n^o contributes the spin and magnetic moment. However, a close look at the structure is necessary.

mass number A = 7

decay of the isotopes:
$_2^7He \rightarrow _2^6He + n^o$
$_3^7Li$ stabil
$_4^7Be \rightarrow _3^7Li + \gamma$

Fig. 3.4: *core structure of Lithium $_3^7Li$.*
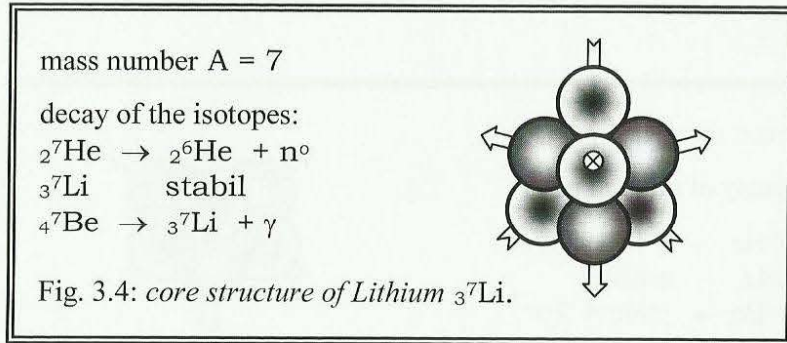
Three α-particles are immediately recognizable within the structure of this most important of the lithium nuclei. If one is removed, there remain 2 n^o and one p^+. For an approximate validation, we first sum up the magnetic moments while ignoring angles and stray fields:

$$(\mu_{He} + 2\mu_n + \mu_p)/\mu_N = -2 - 2 \cdot 2 + 3 = -3 \qquad (3.2)$$

Through vectorial addition of the actual values, one will further approach the measured value (=3,25). In the same manner, one can check the rotation angle ξ predetermined by the structure.

3.3 Beryllium nuclei (with A = 8 and 9)

We add yet another proton and get the light alkaline earth metal beryllium. The alpha-particle model could have firstly been validated by the nucleus of mass number A = 8, as it consists of exactly two α-particles (of A = 4 each). But that's not going to happen.

If this nucleus is created artificially, the α-nuclei change their rotation angle to $\xi = 90°$ and become diamagnetic. They simply do not take notice of one another magnetically, yet are repelled electrically and decay quickly into – how could it be otherwise - 2 α-particles. The spin is zero as expected.

mass number A = 8

decay of the isotopes:
$_3^8Li \rightarrow _4^8Be + e^-$
$_4^8Be \rightarrow 2\alpha$
$_5^8B \rightarrow _4^8Be + e^+ + \nu_e$
$_6^8C \rightarrow _4^6Be + 2p^+$

Fig. 3.5: *core structure of Beryllium $_4^8Be$.*
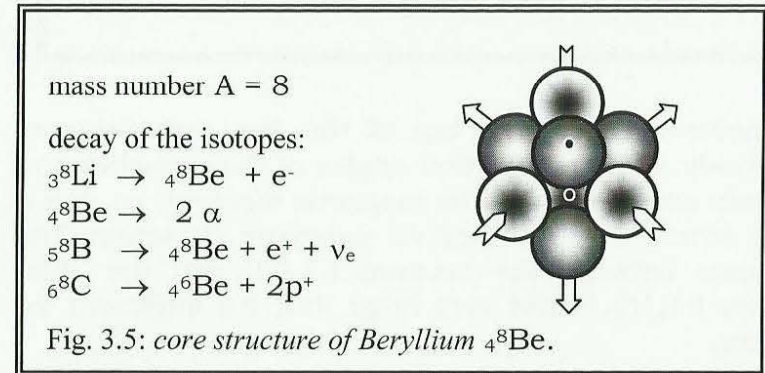
Under these unfortunate circumstances, not even the aesthetically pleasing structure incorporating even α-particles does not help.

A glance at the isotope decay makes clear that $_4^8Be$ is created from $_3^8Li$ when an n^o releases its inner e^- or from boron $_5^8B$, in which case an e^- is captured. This is the first time a neutrino ν_e, acting as some kind of

obstetrician, makes its entry. We will discuss its function later.

The first stable beryllium nucleus is only that with a mass number of 9.

mass number A = 9

decay of the isotopes:

$_3^9Li \rightarrow \; _4^9Be \; + e^-$

$_4^9Be \rightarrow$ stabil

$_5^9B \rightarrow \; _4^8Be + p^+$

Fig. 3.6: *core structure of Beryllium $_4^9Be$.*
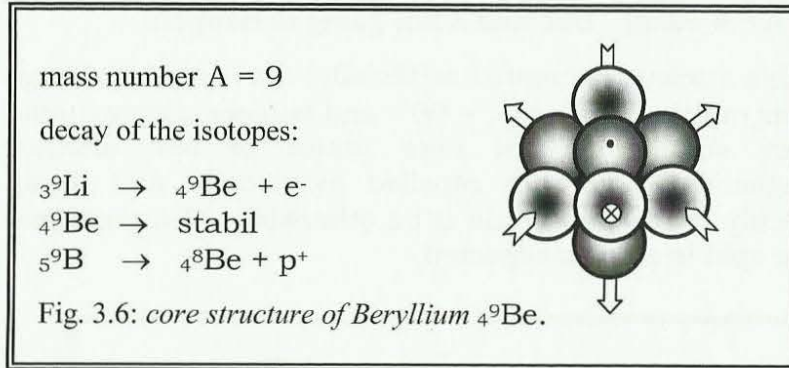
The neutron placed on top of the two α-nuclei may apparently alter the rotation angles of the α-particles to a certain extent through its magnetic moment, so that a stable structure is attained via magnetic attraction. The difference between the neutron (-1,93) and the $_4^9Be$-nucleus (-1,18) is not very large, but it's sufficient for stability.

Bombardment with α-particles makes it clear that high cohesion can only be provided by 3 or more such quartet-structures:

$$_4^9Be \; + _2^4\alpha \; \rightarrow \; _6^{12}C \; + n^o \qquad (3.3)$$
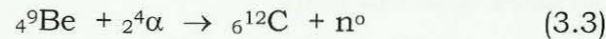
3.4 Bor nuclei (with A = 10 and 11)

5 protons and 5 neutrons allow for a nucleus incorporating the α-structure 8 times while rotating at an angle of ξ = 60°.

mass number A = 10

decay of the isotopes:

$_4^{10}Be \rightarrow \; _5^{10}B \; + e^-$

$_5^{10}B \rightarrow$ stabil

$_6^{10}C \rightarrow \; _5^{10}B + \gamma$ $\nearrow e^+ \searrow \nu_e$

Fig. 3.7: *core structure of Bor $_5^{10}B$.*
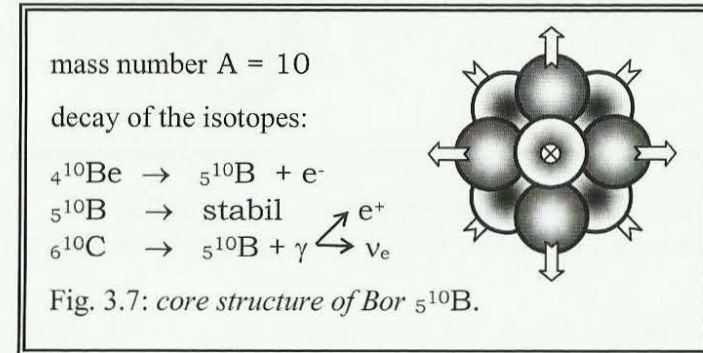
But the harmony is deceiving. This configuration would exhibit the same instability as the beryllium nucleus ($_4^8Be$). An immediate decay into 2 α-particles would be expected.

In this case, there exist additional degrees of freedom, however, which 20% of the boron nuclei take advantage of, even though the resulting structures might appear less harmonic.
The spin of s = 3 can only be caused by 6 nucleons, one half p^+ and the other n^o. What remains is an α-nucleus. But there remain questions, especially in regards to the influence of the utilized measuring devices.

We can possibly resolve the structure better when the additional neutron is once again removed from the most abundant nucleus $_5^{11}B$ (with an occurence of 80%). In any case, the nuclear structure of $_5^{11}B$ allows for a higher packing density, as fig. 3.8 makes clear..

mass number A = 11

decay of the isotopes:

$_4^{11}\text{Be} \rightarrow {}_5^{11}\text{B} + e^-$

$_5^{11}\text{B} \rightarrow \text{stabil}$

$_6^{11}\text{C} \rightarrow {}_5^{11}\text{B} + e^+ + \nu_e$

Fig. 3.8: *core of Bor* $_5^{11}\text{B}$.
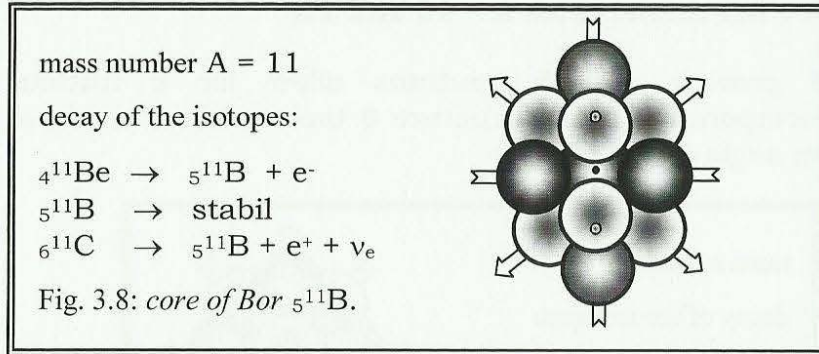
Who can find the most α–structures? I counted 6.

If we remove two of them, one proton and two neutrons remain.

The spin is thus $-s = 3 \cdot \frac{1}{2} = 1,5.$ (3.4)

Regarding the magnetic moment, the two neutrons compensate for the equally large moments of the two helium nuclei $_2^4\text{He}$. The remainder is a small differential and the magnetic moment of the proton, not excluding stray fields:

$$(2\mu_{\text{He}} + 2\mu_n + \mu_p)/\mu_N = 2 \cdot 2 - 2 \cdot 2 + 3 = 3 \qquad (3.5)$$

or, with the measured values:

$$= 2 \cdot 1,88 - 2 \cdot 1,93 + 2,79 = 2,68 \qquad (3.6)$$

Now, the nucleus only lacks a proton in order for this magnetic moment to vanish. This yields the ideal structure of the carbon nucleus $_6^{12}\text{C}$.

3.5 Carbon nuclei (with A = 12 to 14)

With 6 protons and equally many neutrons, three α-particles can be formed and stacked upon another in a twisted manner. Consequently, the middle layer adapts a rotation angle of $\xi = 0°$ and thus generates a two-fold magnetic moment. This in turn is compensated by the two outlying α-particles, which change their respective angle ξ accordingly.

Spin is negated also. This case validates the alpha-particle model of vortex cores indeed.

The relatively high mass defect is caused mostly by the central α-particle, which, wedged between the other two, is being forced into a $_2^4\text{He}$-structure. With an angle of $\xi = 0°$ its mass decreases.

mass number A = 12

decay of the isotopes:

$_5^{12}\text{B} \rightarrow {}_6^{12}\text{C} + e^-$

$_6^{12}\text{C} \rightarrow \text{stabil}$

$_7^{12}\text{N} \rightarrow {}_6^{12}\text{C} + \gamma \searrow \nu_e$

e^+

Fig. 3.9: *core structure of Carbon* $_6^{12}\text{C}$ ($_6^{13}\text{C}$ dashed line).
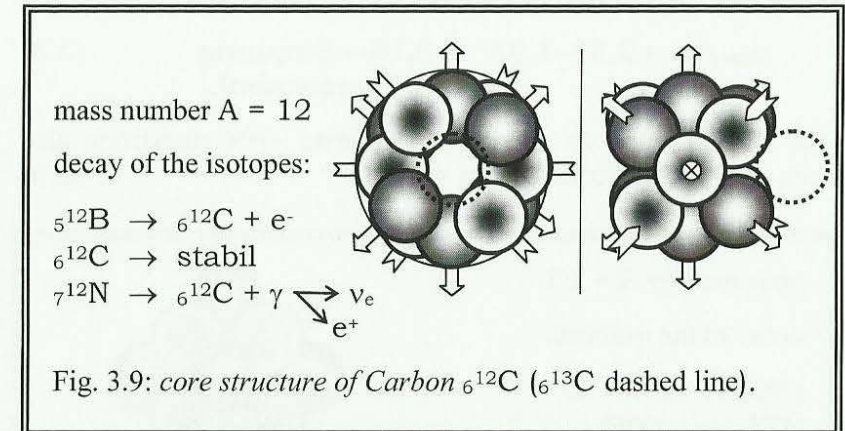
The carbon isotope $_6^{13}\text{C}$ is stable as well. It absorbs a neutron in front of "its hole" (fig. 3.9, on the left) and thus assumes its spin ($s = -\frac{1}{2}$).

There is room for another neutron on the exact opposite side. With an inversed spin axis, it fully negates the spin once again ($_6^{14}$C). Only loosely coupled can ß-decay occur.

Thus the isotope $_6^{14}$C, of relevance to carbon dating, is no longer stable and releases an electron from one of its attached neutrons every 5730 years:

$$_6^{14}C \rightarrow {}_7^{14}N + e^- \tag{3.7}$$
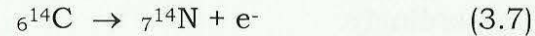
3.6 Nitrogen nuclei (with A = 14 and 15)

Within the nitrogen nucleus $_7^{14}$N, produced from the carbon isotope $_6^{14}$C, one of the two n° has now been converted to a p⁺ due to the loss of its inner electron. Therefore, the magnetic moment is reduced to

$$\mu_{ges}/\mu_N = 2{,}68-1{,}93 \quad = 0{,}75 - \text{Streuung} \tag{3.8}$$
$$= 0{,}4 \text{ (gemessen)}.$$

The equally stable nitrogen nucleus $_7^{15}$N assumes the spin of the additional n° (s = – ½). (3.9)

mass number A = 15

decay of the isotopes:

$_6^{15}C \rightarrow {}_7^{15}N + e^-$
$_7^{15}N \rightarrow$ stabil
$_8^{15}O \rightarrow {}_7^{15}N + e^+ + \nu_e$
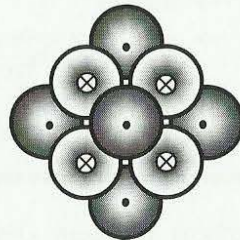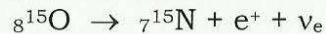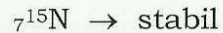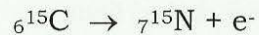
Fig. 3.10: *core structure of Nitrogen $_7^{15}$N.*

This structure looks the same from all sides. And for the first time, a layering becomes visible. 5 protons that are not touching are found in the middle layer. Above and below, 4 neutrons are spinning in opposite directions, respectively. An additional proton is situated at both the top and bottom tips.

All nucleons need to unify their spin and unroll along the 45° latitude for frictionless operation. Through the intertwinement of a cubic neutron lattice and a cubic proton lattice, a packaging of high density is attained. This is the prime directive especially when it comes to the construction of large nuclei.

One could call it vortex-layer or spherical shell model [4]. Anyway, it supercedes the "hedgehog", that can be constructed with only a few nucleons. What remains is the generally persistent alpha-particle model.

3.7 Oxygen nuclei (A = 16 to 18)

The image of the *oxygen* nucleus $_8^{16}$O is reminiscent of the *carbon* nucleus $_6^{12}$C (fig. 3.9). This time, we're dealing with 4 stacked α-particles already. Therefore, not only one, but two of them are sandwiched in the middle which, as already mentioned, results in an increased mass defect.

The noble gas *neon* $_{10}^{20}$Ne already has 5 α-layers, appearing very compact spatially. The nuclei of *magnesium, silicium, sulphur* and *calcium* follow the same scheme.

Carbon	$(_6{}^{12}C$	with 3 α-layers)
Oxygen	$(_8{}^{16}O$	with 4 α-layers)
Neon	$(_{10}{}^{20}Ne$	with 5 α-layers)
Magnesium	$(_{12}{}^{24}Mg$	with 6 α-layers)
Silicium	$(_{14}{}^{28}Si$	with 7 α-layers)
Sulphur	$(_{16}{}^{32}S$	with 8 α-layers)
Argon-Isotope	$(_{18}{}^{36}S$	with 9 α-layers)
Calcium	$(_{20}{}^{40}Ca$	with 10 α-layers)

These elements are all special insofar as the number of protons is equal to the number of neutrons within their nuclei. They thus possess an integral number of complete α-layers, the properties of which they inherit.

With every layer, the mass defect increases. As both ends of the increasingly tube-like nuclei have less and less influence on mass, the mass defect approaches a boundary value which is reached by the iron nucleus $_{26}{}^{56}Fe$. Even larger nuclei again experience decreasing mass defects while the deformation of the α-layers also diminishes with increasing package density.

The possible attachment of nucleons at the ends of the α–tube, as already discussed for carbon, also occurs in other nuclei consisting of α–layers. In these cases, not only decay series, but also spin and magnetic moment are often times identical.
For example, n°-absorption results in the same spin in case of $_6{}^{13}C$ (attached to $_6{}^{12}C$) or at the opposite pole in case of *fluorine* $_9{}^{19}F$.

This explains the rule that uneven nucleon counts always exhibit a half-integral spin.

3.8 Metrological obstacles of verification

The law of unipolar induction

$$\mathbf{E} = \mathbf{v} \times \mathbf{B} \tag{1.2}$$

relates the electric field E (in our case the electric charge), the velocity v (or spin), and the magnetic field (or flux density) B via the process of induction.

Therefore, it makes sense to utilize measuring devices, for example based on optical methods, which do not influence the values to be measured.

Conversely, it makes little sense to expose the target objects to extremely strong magnetic fields, as is often the case (e.g. in atom beam resonance experiments for measurement of nuclear moments according to Rabi). While one arrives at certain values, there is no guarantee for their authenticity.

Rather, there's a risk of merely detecting the measuring device's perturbations. This systematically violates the principle of minimal influence upon the values to be measured by the measuring apparatus itself.

In practical nuclear physics, the inner nuclei mainly consisting of α–layers appear nearly unphased by strong external fields. Only the less integrated nucleons situated towards the open ends freely follow the field lines of the measurement channel. And as only they contribute measurably to spin and magnetic moment, they occasionally display a truly spectacular performance.

They roll to the opposite side, causing a spontaneous spin reversal, or form chains consisting of up to 9 nucleons (i.e. with a high spin of

$$s = 9 \cdot \tfrac{1}{2} = 4{,}5 \qquad (3.10)$$

in the case of, for example, niobium $_{41}^{93}$Nb, strontium $_{38}^{87}$Sr, krypton $_{36}^{83}$Kr, or germanium $_{32}^{73}$Ge).

To clarify, we take a look at the different, yet stable germanium isotopes. In its 16 α-layers, all 32 protons and neutrons are incorporated in equal amounts. That leaves us with 9 neutrons, which form a chain of such length (with s = 4.5) through polar coupling within an external magnetic field.

Only in this way can the spin (s = 3) of the boron nucleus $_5^{10}$B generated by 6 nucleons be explained. This doesn't imply, however, that this peculiar structure exists outside of the measuring arrangement.. Nothing can keep the nucleus from transforming into a less energetic state once the strong magnetic fields have been turned off again.

Without question, the nucleon cluster strives towards a spherical shape and maximum compensation in terms of spin and magnetic moment, as demanded by the well-known "liquid drop model".

I don't want to get lost in the vast amounts of known and more or less stable nuclei. Rather, I'd like to focus on the fundamental principles that the vortex model of nuclear physics offers.

4. The vortex model of nuclei

We have to part with the "hedgehog model", in which the spin axes of the nucleons are pointing in all directions. This configuration only appears in small nuclei, at boundaries, or at the ends of tubular nuclei consisting of stacked alpha-particles.

In medium and heavy nuclei, there is more order. Only when all spin axes are parallel can the high packing density demanded by the "liquid drop model" be attained.

As another ordering mechanism, layers of homogenous nucleons appear, allowing the definition of proton and neutron layers, comparable to the conventional shell model (fig. 3.10). In addition, the nucleon cluster is supposed to be striving towards a spherical shape, so that singular rotation shells can emerge and rotate with a unitary frequency.

The layer model of spherical vortexes presented here confirms the known fact that the nucleon count A determines whether the overall spin is integral or not. This remains applicable even when spin reversal should occur due to strong external magnetic fields.

An example for the spin reversal of s = 0 to s = 1 is fluoride $_9^{18}$F when the spin of p$^+$ and n$^\circ$ are added.

On top of that are the construction rules that we have derived for alpha-particles, which are present in nearly all nuclei.

4.1 The rules of nuclear construction

With every α–layer, the magnetic moment increases. This has several consequences:

1. the inner bonding force of the nucleus increases,

2. the magnetic north pole on the one end and the magnetic south pole on the other end are strengthened,

3. further nucleons are increasingly attracted by the magnetic poles,

4. which in turn attract more nucleons,

5. especially neutrons (due to the protons' mutual electric repulsion).

6. Free nucleons form chains,

7. which strive to close the magnetic circuit with their magnetic counter-pole.

8. The higher the packing density, the more they contract one another through their fields,

9. the more nuclear radius decreases.

10. Only the inner structure of the nucleons is responsible for the mass defect.

11. The nuclear bonding force is purely magnetic,

12. and only effective over the small distance to neighboring nucleons,

13. meaning nucleons hold on „to each other",

14. explaining the cohesion of small nuclei,

15. but also the decay of large nuclei,

16. once centrifugal force and electric repulsion become dominant.

4.2 The radius of the nucleus and the halo nuclei

It would be bad for rules to have only limited applicability, for example to light nuclei, only to lose their validity when it comes to heavier ones.

Let's take a look at the rules 8 and 9 regarding the size of nuclei and their incorporated nucleons. Experimental results suggest a rather diffuse surface, allowing only for approximate values for the nuclear radius.

The approximation that a total of A nucleons, as small spheres of the volume $\qquad V = A \cdot (4\pi/3)R_N^3 \qquad (4.1)$

fit into the volume of another spherical nucleus $\qquad V = (4\pi/3)R_K^3 \qquad (4.2)$

given constant charge density leads to the simple and common relation: $\qquad R_K = R_0 \cdot A^{1/3} \qquad (4.3)$

But the packing density of the sphere cluster can not be particularly high. Specifically, less than 68% of the nucleus' volume are occupied by the nucleon vortexes [4]. In addition, certain distances need to be respected to allow for the contact of equally oriented neutrons only.

The experimental domain suggests the value:

$$R_N < R_0 \approx 1{,}2 \ldots 1{,}4 \text{ fm} \qquad (4.4)$$

But how are the nucleons supposed to remain rotating under this textbook-like approach? This would require

$$R_0 > (1/0{,}68)^{1/3} \cdot R_N = 1{,}27 \text{ fm} \qquad (4.5)$$

This case $\qquad R_0 = R_N = 1{,}11 \text{ fm} \qquad (4.6)$ describes something akin to *"square tomatoes in a box too small"*. Yet it is precisely this extreme condition preventing any rotation that is satisfied by the lighter nuclei, above all the helium nucleus.

At this point, modern nuclear physics finds itself with its back against the wall, having to employ a factor in its calculations that leaves only one conclusion: *"something must have shrunken the nucleons!"*

And indeed, the field dependency of length measurements derived in Volume [2] on potential vortexes has an effect ([2], Gl.2.20, S. 27):

$$E, H \sim 1/r^2 \qquad (4.7)$$

The only permissible and correct explanation lies in the electric and magnetic fields of the nucleons. Through their fields, they mutually reduce each other's size. The dimensions determined by the field not only explain the size of nuclei, but also the field effect of particles known as gravity, as well as the accommodation of a much larger electron within a neutron, where the field lines converge and thus result in extremely high field strengths.

Conversely, nuclei expand vastly if for example two loosely attached additional neutrons create a "halo". They remain magnetically bound to the nucleus, yet rotate with higher velocities due to the increased radius. This calls for a great respect distance under weakened field conditions and lets the neutron radius incease even further.

In this way, the halo nuclei of lithium $_3^{11}$Li up to carbon $_6^{19}$C reach the nucleus dimensions of lead $_{82}^{208}$Pb, and thus come close to the limit of stable nuclei.

4.3 Spherical nuclei

30 years ago already, the then nuclear research center in Karlsruhe publicized experimentally determined dimensions and shapes of various nuclei, which was reported on by "Bild der Wissenschaft" [6]. Apart from the obvious spherical shape, cylindrical and elliptical nuclei had also been found.

Such experimental results are very valuable as a back check for the nucleon puzzle and indispensable for anyone enjoying the recreation of the shapes found with nucleons [4, 7]. Not only the number of p$^+$ and n^o involved, but also spin, direction of rotation, and nuclear cohesion through magnetic moment need to fit together, whereby even "remote" p+ on opposite ends of the nucleus still require a magnetic attraction greater than the electric repulsion caused by similar charge.

I will pick three examples from the plethora of possibilities [4].

The structure of the oxygen nucleus $_8^{16}$O, for which a spherical shape of radius R_O = 3,3 fm is cited, has been explained already. It corresponds in large part to the carbon nucleus $_6^{12}$C, as depicted in Fig. 3.9, incorporating 4 instead of 3 alpha-structures, however.

Its mean dimensions in the three spatial coordinates, taken from fig. 3.9. and eq. 4.6 are, according to the

vortex model: $\qquad R_O = 2,97 \; R_N = 3,29$ fm $\qquad (4.8)$

in comparison to measurement: $\qquad R_O = 3,3$ fm . $\qquad (4.9)$

The sought after spherical shape will become more efficient with increasing nucleon count, e.g. in case of the calcium nucleus $_{20}^{40}$Ca.

In the graphical representation (Fig. 4.1), all rotation axes are largely parallel, with all n° (in light color) assumed to rotate clockwise while all p⁺ (in dark color) are rotating counterclockwise.
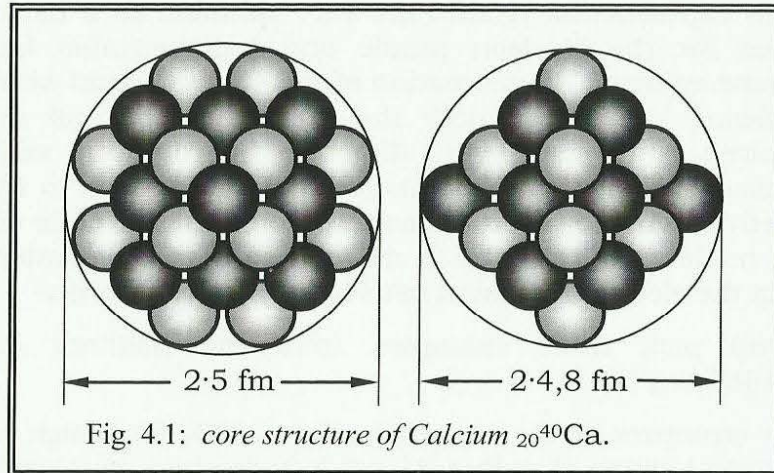
Fig. 4.1: *core structure of Calcium* $_{20}^{40}$Ca.

If the calcium nucleus is measured {{modelled?}}, the vortex model yields a radius of approximately 4.9 fm while staying close to a spherical base shape.

Actual measurements yield a spherical structure of a radius R_{Ca} = 4.4 fm [6]. But if the sphere as a whole has shrunk, each nucleon should, due to increases in field strength, also have been reduced in size respectively; i.e. The nucleon radius has decreased by

11% of R_N = 1,11 fm to R_N = 1,0 fm   (4.10)

To validate this interesting result, further examples are to be examined.

4.4 Elliptical nucleus shapes

The experimental findings for the magnesium nucleus $_{12}^{26}$Mg yielded the shape of an ellipse [6] of the radii 5.9 fm (major axis) and 3.0 fm (minor axis).
What values does the vortex model provide for this example?
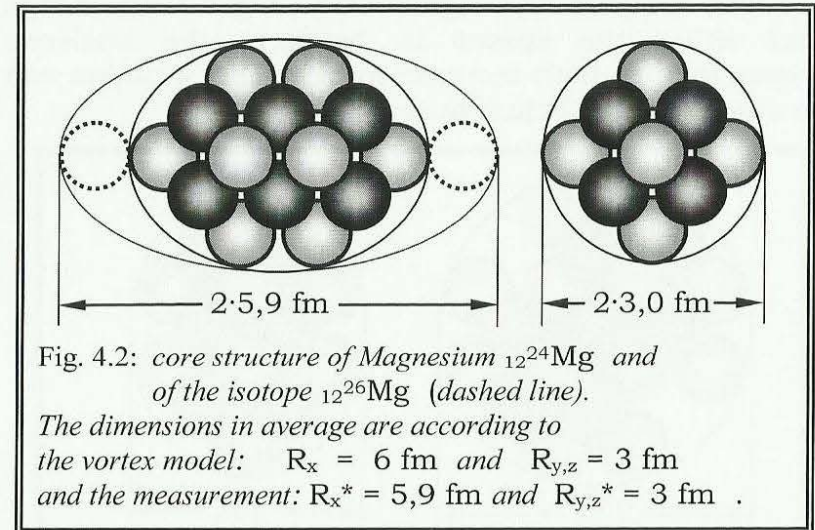
Fig. 4.2: *core structure of Magnesium* $_{12}^{24}$Mg *and of the isotope* $_{12}^{26}$Mg *(dashed line).*
The dimensions in average are according to the vortex model: R_x = 6 fm *and* $R_{y,z}$ = 3 fm *and the measurement:* R_x^* = 5,9 fm *and* $R_{y,z}^*$ = 3 fm .

The graphic firstly displays the most abundant (79%) naturally occurring nuclear structure of magnesium $_{12}^{24}$Mg. It comes very close to a spherical shape. All positions are occupied and thus a high packing density achieved.
If two more neutrons are added, they will attach themselves at both ends, as uncompensated magnetic fields are pointing outwards there. It is exclusively at these locations that the magnetic attractive forces is at a maximum, resulting in a notably elongated structure in the case of the magnesium isotope $_{12}^{26}$Mg.

Comparing the dimensions predicted by the vortex model to the measured values, we find that once again, the radius of the nucleons has been diminished according to Eq. 4.10. Only with R_N = 1.0 fm do the values match the measured results.

This is different for nuclei with unoccupied spaces. They are less compact and significantly larger. This means that either the spaces in between, the nucleons themselves, or both increase in size. The situation can be studied with silicium nuclei.
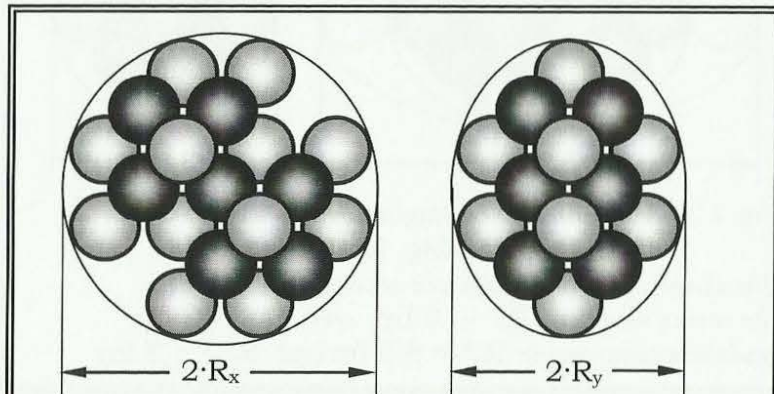
Fig. 4.3: *core structure of Silicium $_{14}^{28}$Si.*

The dimensions in average are according to the vortex model: R_x = 5,1 fm *and* $R_{y,z}$ = 3,8 fm *and the measurement:* R_x^* = 5,5 fm *and* $R_{y,z}^*$ = 4,0 fm .

Silicium therefore presumably features the common radius of singular nucleons (R_N = 1.11 fm).

If both shape and dimensions of model and measurement agree as shown, we can't be very far off the mark.

4.5 Vortex-shell model

Let us once again direct our attention towards layers occupied by nucleons, as exhibited by heavy nuclei especially. A comparably clear case appears to be the well populated sulphur nucleus, on the basis of which I would like to elaborate on the theses of the vortex-shell model.
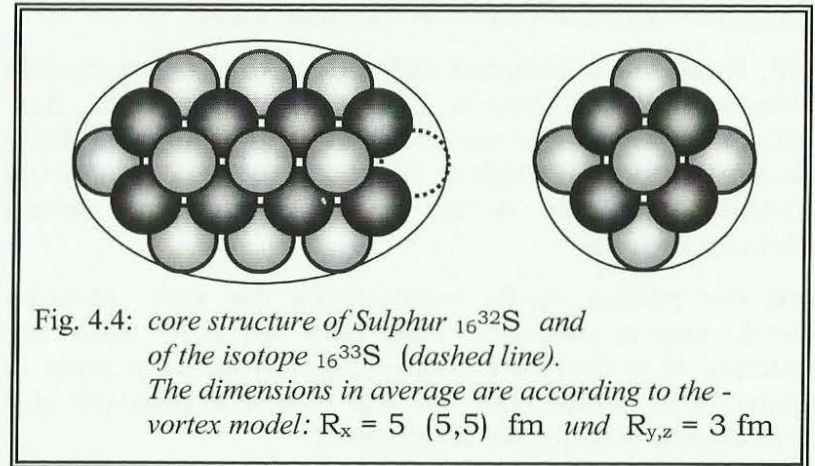
Fig. 4.4: *core structure of Sulphur $_{16}^{32}$S and of the isotope $_{16}^{33}$S (dashed line). The dimensions in average are according to the - vortex model:* R_x = 5 (5,5) fm *und* $R_{y,z}$ = 3 fm

Here we find a central layer in the middle occupied by 10 (or more) neutrons. On both sides, 8 protons form independent layers terminated by 3 neutrons each, respectively.

Of course there is no obligation to fully fill up each layer, but the drive towards a spherical shape and a high package density does favor it.

Additionally, symmetry relative to a rotation axis is required, so that there is no imbalance.

Whoever was raised on the "shell model", like my generation, will look at the pictured sulphur nucleus from the front and immediately recognize the sought

after shells. The innermost one is occupied by neutrons, the next one by protons and the outermost one once again by neutrons. This is indeed reminiscent of the atomic shell's structure, only in this case with much smaller distances.

The distribution of protons and neutrons in the shells is most probably such that each shell's center of mass is coincident with the center of the nucleus [4].

Still, there are significant differences to the two models hitherto utilized, which postulate more than they explain. However, the most important difference is likely the explanation of nuclear bonding by the forces of the existing magnetic fields, without invoking strong interaction at all.

Now the proton, while maintaining the same rotation speed, has a magnetic field 50% stronger than the neutron. It is therefore nearly impossible for a layer of neutrons to compensate for the magnetic moment of a layer similarly occupied by protons.

In the images of light nuclei shown, this only plays a minor role, as the comparably short distance from a north to its associated south pole remains surmountable. Here, parity between protons and neutron $(Z = N)$ dominates, although additional neutrons can be helpful, as is sometimes the case beyond the atomic number $Z=3$ and a general rule for medium nuclei.

Heavy nuclei tend towards a ratio of $Z/N = 3/2$, and some nucleons close to the stability boundary indeed match it, e.g. $_{80}^{200}Hg$, $_{78}^{195}Pt$, $_{76}^{190}Os$, $_{72}^{180}Hf$, or $_{68}^{170}Er$.

4.6 Karlsruhe nuclide chart

In the nuclide chart published by the Karlsruhe research center, this transition drawn in between the two limiting curves $(Z/N = 1$ and $3/2)$ becomes very obvious [8].
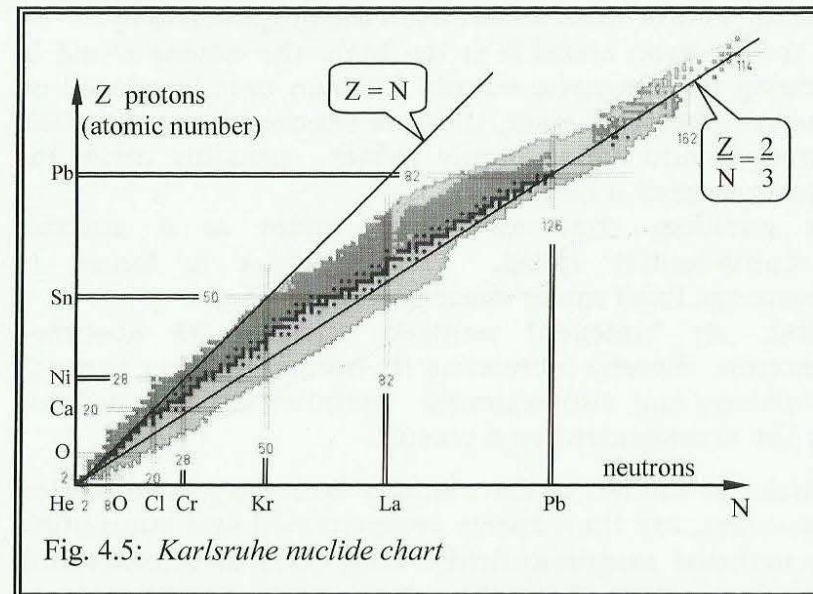
Fig. 4.5: *Karlsruhe nuclide chart*

It remains exciting when it comes to heavier elements, especially rare earths, as on the one hand they have too few neutrons to fully compensate the magnetic field, and on the other hand are so large that field lines can no longer be closed. Thus, they turn into strong permanent magnets.

Representative of this are neodymium ($_{60}Nd$) or samarium ($_{62}Sm$), for example. These nuclei align their parallelly configured spin axes to externally applied magnetic fields.

The nuclide chart is supposed to illustrate the fine line on which stable nuclei of the periodic system are situated, where additional, mostly unstable isotopes are to be found, and where the stability boundary ultimately lies.

From the perspective of the vortex model, the stability of nuclei can be determined from the graphic thusly:
If the neutron count N is too high, the excess n^o aid in closing the magnetic circuit, but can only be placed on the periphery. As such, they are exposed to a lesser field strength and consequently inflate, possibly up to the dimensions of a halo.
In addition, they no longer rotate at a suitable circumferential speed. The nucleus is forced to rearrange itself under these circumstances.
First, an "unloved" neutron releases its absorbed electron, thereby increasing its atomic number through ß⁻-decay, and subsequently assumes its new position in the arrangement as a proton.

Nuclei to the left of the stability boundary have too few neutrons, are thus barely compensated and susceptible to external magnetic fields. They tend to interact with passing neutrinos, thereby gaining the energy required for their rearrangement (ß⁺-decay) and emit a positron. Alternatively, they release protons or even whole α–particles from their nucleon cluster.

If a stable state is still not attained afterwards, the rearrangement continues. These processes are well-known from technical literature as decay series.
We can summarize: The nucleus knows how to help itself!

4.7 Radioactivity

In case of natural radioactivity, α– or ß–decay only occurs when a superheavy nucleus tries to reach the "valley of stability". Take the decay series of uranium nuclei for example:

$$_{92}{}^{238}U \xrightarrow{\alpha} {}_{90}{}^{234}Th \xrightarrow{\beta^-} {}_{91}{}^{234}Pa \xrightarrow{\beta^-} {}_{92}{}^{234}U \xrightarrow{\alpha} {}_{90}{}^{230}Th \xrightarrow{\alpha}$$

$$\rightarrow {}_{88}{}^{226}Ra \xrightarrow{\alpha} {}_{86}{}^{222}Rn \xrightarrow{\alpha} {}_{84}{}^{218}Po \xrightarrow{\alpha} {}_{82}{}^{214}Pb \xrightarrow{\beta^-} {}_{83}{}^{214}Bi \xrightarrow{\beta^-}$$

$$\rightarrow {}_{84}{}^{214}Po \xrightarrow{\alpha} {}_{82}{}^{210}Pb \xrightarrow{\beta^-} {}_{83}{}^{210}Bi \xrightarrow{\beta^-} {}_{84}{}^{210}Po \xrightarrow{\alpha} {}_{82}{}^{206}Pb$$

or:

$$_{83}{}^{210}Bi \xrightarrow{\alpha} {}_{81}{}^{206}Tl \xrightarrow{\beta^-} {}_{82}{}^{206}Pb$$
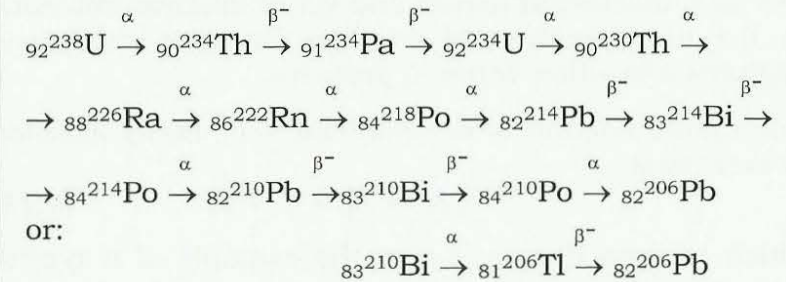
Fig. 4.6:   *decay series of uranium $_{92}{}^{238}U$ to Lead $_{82}{}^{206}Pb$.*

In this instance, the nucleus rearranges itself 14 times. The interval between rearrangements can be years or mere fractions of a second. Until a stable lead nucleus is eventually produced, the structures of various heavy nuclei appear (thorium, radium, radon, bismuth, etc.), which shed light on the inner arrangement of the nucleons through the observable rearrangement measures.

By evaluation of the known radioactive decays, the construction schemes of nuclei can be verified.. This is not the place to elaborate all of it in detail, but still the effort shall be rewarded, for more confirmations of the vortex model await ([4]: according to the MFT).
For now, I want to discuss the origin of radioactive radiation.

α–radiation is well understood: A nucleus loses four nucleons, which are bound tighter to each other than to the nucleon cluster at large, at once, despite them coming from three different layers stacked on top of one another. The effect, range, and other properties of α–radiation are exhaustively covered in lexica and textbooks.

New as a theoretical aspect and yet of decisive influence on the determination of bonding forces is solely the magnetic attraction between particles.

Much more difficult to comprehend is β^-–decay assisted by neutrinos:

$$_0^1n \rightarrow {}_1^1p + e^- + \overline{\nu}_e \quad , \qquad (4.11)$$
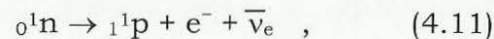
Which we can discuss using the example of a typical β^-–emitter:

$$_{79}^{198}Au \rightarrow {}_{80}^{198}Hg + e^- + \overline{\nu}_e \qquad (4.12)$$
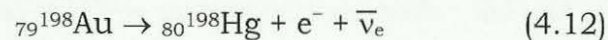
Specifically, the question is: "How can an electron escape from the interior of a neutron?"

Both are spherical field vortexes, and what's whirling is neither matter, fine-structured matter or quark-like. It is merely electric and magnetic fields, by which the particles define themselves.

It is the same fields that structure themselves under the vacuum pressure of potential vortexes, that control the accumulation and superposition of field vortexes and that are responsible for the construction and decay of nuclei thanks to the electromagnetic interaction.

The same should hold true for the so-called "weak interaction", even though it is of a magnitude 10^{11} times lower.

4.8 Oscillating interaction

The weak interaction, which plays a role all the way from the already discussed radioactive decay of heavy nuclei to beta-decay, is increasingly being discussed in relation to the electromagnetic interaction (Glashow-Weinberg-Salam model, 1979 nobel prize for physics). And I may add: the weak interaction isn't at all different from the electromagnetic interaction, both being inextricably linked with the oscillating electric fields of neutrino radiation.

According to the vortex model, a neutrino is created out of an electron whose rotation has been accelerated until its spherical vortex has turned into a ring vortex. This leads to a series of consequences, the sum of which confirm all properties of neutrinos most impressively:

1. The neutrino ν_e loses its local dependence, as it no longer possesses a vortex center at which all field lines must converge (and $c = 0$ because of $E \sim 1/c^2$).

2. As a ring vortex, the ν_e is perpetually turning inside out in a barely measurable high frequency oscillation.

3. On average, the ν_e has no electric charge, as in one moment, its charge is negative (e^-), the next moment positive (e^+), etc.

4. On average, the ν_e has no mass, as in one moment, it exists as matter (e^-), turning into antimatter (e^+) in the next.

5. Devoid of interactions, the ν_e exhibits its well-known permeability.
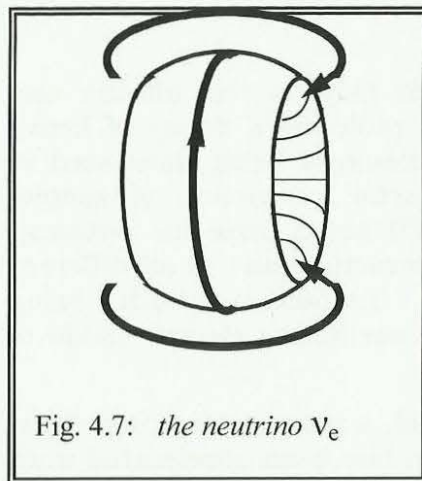
Fig. 4.7:   *the neutrino* ν_e

So what causes the effect of the "weak interaction", itself about 10^{13} weaker than the non-existent "strong interaction"?

As an oscillating particle, the neutrino can unimpededly approach a neutron to suddenly strike by means of its magnetic force, as it possesses a magnetic moment, being a rotating particle of spin s = ½. Its perpetually polarity switching electric fields rattle and tear at the neutron, which, due to its charge distribution, offers sufficient opportunity for interaction to eventually forfeit its inner electron.

Nothing else is to be expected from an electron within a neutron than that it would react to electric fields outside of the vortex boundary. If the sum of the E-fields causes a strong attraction, it will be pulled right out of the neutron's pole.

This leads to an increase of the neutron's radius, thereby losing mass and energy. The decay equation (4.11) reflects this by the emission of an anti-neutrino. This is equivalent to the absorption of a neutrino ν_e, which would have to be added to the n^o on the left side. Considering the negative sign of the neutrino's mass, this measure becomes mandatory, even (see [2], p.72 et seq.), at least as soon as the scientific community accepts that these particles travel faster than light [9].

The "discovered" violation of parity conservation [10] is thus explained completely.

The neutrino, in the course of its oscillating electromagnetic (so-called "weak") interaction, contributes its half-integral spin and thus alters the entire spin balance. If it reverses rotation during decay, it nonetheless remains a neutrino and does not at all turn into an anti-neutrino. Such a hypothetical particle may obviously not exist, as the neutrino itself is constantly oscillating between the states of matter and antimatter.

And so, the interpretation suddenly makes sense: Autonomously, i.e. without external assistance of an approaching neutrino, the nucleus is incapable of releasing the electron. In addition, the neutrino is required to maintain balance of energy and momentum, for which it is particularly suited thanks to its special properties (for more details see Potential Vortexes vol. [2] p. 76 et seq. and vol. [3] p. 90 et seq.).

This connection was known to Nikola Tesla over a century ago already, tempting him to exclaim: "If only we could effectively deflect neutrino radiation, there would be no radioactivity on this Earth." [11].

5. Vortex model of the atomic shell

Both the calculation of elementary particles presented in volume [3] as well as the physics of atomic nuclei can be informally derived from a vortex model based on only one type of interaction, in accordance with the unification theory discussed in volume [2]: That of the electric and magnetic fields.

When speaking of observably attractive forces between two bodies, of strong and weak interaction, or of gravity, "bodies" really mean structured collections of field vortexes, closing the distances between each other through their field interactions, which is being interpreted as an attractive force according to the relation derived (1.3):

$$E, H \sim 1/r^2 \qquad (4.7)$$

Considering the perfect agreement between vortex description and measurable reality, terms like mass, charge, gravity, etc. by now appear as mere make-shift descriptions.

Admittedly, we are unable to observe the field dependency of radii and linear dimensons according to the proportionality formulated in 5.1, as they influence velocities and, by way of the speed of light c, also our observation itself. Only with the objectivity theory derived in [2] and [3] can we overcome this deficiency.

A model yielding such success for elementary particles and atomic nuclei should be suitable for describing the atomic shell as well.

5.1 The classical view of hydrogen

In the classical model of the hydrogen atom, Coulomb's law describes the force that the proton exerts upon the electron situated within the shell:

$$F = \frac{-e_o \cdot e_o}{4\pi\varepsilon_o} \cdot \frac{1}{r_H{}^2} = -8,24 \cdot 10^{-8} \ [N] \qquad (5.1)$$

This force emerges consequently to the elementary charge e_o of opposite polarity. In the Bohr model, this would correspond to a circular orbit of radius $r_H = 53$ [pm], the basic state of an electron in a hydrogen atom.

In graphical terms, the electric field lines run from the nucleus to the negatively charged shell electrons. But when looking for the electron, one can merely make out a diffuse electron cloud – an oscillating electrical charge whirling around the nucleus.

The mathematical foundation of this is provided by the Schrödinger equation, an eigenvalue equation, the solutions of which are supposed to describe the probability density of the no longer existing particle, or so current doctrine claims. Being one the fundamental equations of quantum physics, it remained a postulate, however useful.

Only the discovery of potential vortexes of the electric field and the subsequent respective extension of field theory allowed for the derivation of this highly significant equation [1]. Thus, its origin became clear for the the first time. Without necessitating a postulate and fully derived from the known laws of electromagnetism, it alone determines the structure of atoms, as centrifugal force, gravitation and other force actions are not even part of the new field theory.

5.2 Atomic hydrogen

Assuming spherical symmetry and a homogenously distributed charge, the electric field strength diminishes quadratically from the nucleus and similarly from the electrons distributed within the atomic shell over the distance r:

$$E = \frac{Q}{4\pi\varepsilon_o} \cdot \frac{1}{r^2} \quad \text{so it is:} \quad \boxed{E \sim \frac{1}{r^2}} \qquad (5.2)$$

But conversely, this well-known relation can also be interpreted as "field-dependent length contraction" when assuming that the sphere's radius r, as well as all other dimensions and velocities affected by a field, are determined by it. In this way, all kinds of attractive forces, including gravity [2], can be understood as field effects occurring when one body is located within another's field of influence and vice versa.

In the shell of an atom, an electron is within the field of the nucleus, thereby reducing their distance and "attracting" each other, as we like to say. But shortly before making contact, the electron will notice that at close range, the proton's field disappears (vol. [3], p.76), fortunately preventing the seemingly predetermined crash.

But what became of the electron? On the side facing the nucleus, it is exposed to a much stronger field, causing the local radius to be diminished significantly. It has been deformed into a hemisphere. Meanwhile, its self rotation doesn't seem to interfere at all. Its side facing the nucleus is shrunk at all times.

Proton and electron are counter-rotating, yet display quite different unrolling radii. Consequently, in addition to their self rotation, the uneven pair also rotate quickly around their center of mass. The whole then appears spherical.

With its asymmetric atomic shell, atomic hydrogen holds a special position. Due to the deformation, there's a gap in its electron shell, making the gas highly reactive. It seems likely that the atomic form doesn't even occur under normal circumstances.

Instead, hydrogen reacts especially well with other elements or, if need be, with its own kind to form the gaseous molecule H_2. The molecular form exhibits no magnetic moment, as the atoms have diametrically opposed spin.

5.3 Das 1s-Orbital

All other elements of the periodic system have a nucleus containing two or more protons and a respective number of electrons in their shell. Thus, the nucleus immediately captures an additional electron and deforms it hemispherically, closing the gap in this way. The s-orbital, now fully occupied by 2 electrons, assumes the shape of a complete sphere. Both electrons are counter-rotating and close the magnet circuit inside the spherical shell already, thereby bonding mutually via magnetic forces..

The nucleus is wedged in the middle of the two spherical shells. At this position, the electric fields of similarly charged and therefore repulsing electrons are negated. This particular point devoid of electrical fields even accommodates extended, heavier nuclei without

any harmful contact – under the empirically established constraint that their radius does not significantly exceed 10 fm.
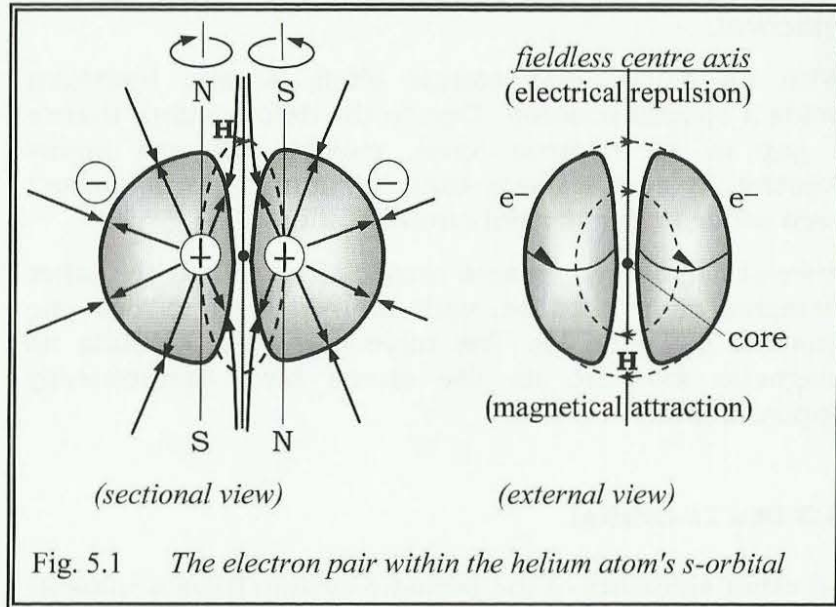
Fig. 5.1   *The electron pair within the helium atom's s-orbital*

If all types of attractive forces can be traced back to a reduction in distance measure, similarly charged electrons should increase their radii conversely due to their repulsion. This conclusively explains why the classical electron radius (r_e = 2.82 fm) is much smaller than the electron pair in the helium atom's shell, by a factor of 10,000.

The merit of both discovering and calculating this enormous growth goes to Niels Bohr.

5.4 The atomic radius of helium (1s-orbital)

Under the inappropriate assumption of a planar circular orbit, the Bohr radius r_1 of the innermost electron orbit (for n = 1) can be calculated:

$$r_n = \frac{4\pi\varepsilon_o \cdot \hbar^2}{m_e e^2} \cdot n^2 \quad \text{und:} \quad r_1 = 53 \text{ pm} \tag{5.3}$$

But the model is only able to describe the behavior of hydrogen atoms and ions with only one electron. According to eq. 5.3, a radius of r_2 = 212 pm can be calculated for the second shell (n = 2).
(for n = 3: r_3 = 477 pm, for n = 4: r_4 = 848 pm, etc.)

Compared to actual measured results, the classically calculated values are off by a factor of >2, however. A reason might be that the field-dependent length contraction, caused by neighboring electrons as well as measurement interference on the scattered particles, is not considered. This mutual influence directly distorts the radius values.

Only in formation with other atoms does an atom's radius become repeatedly measurable. Referred to as "covalent radius", it also signifies the minimum distance of neighboring atoms. For this reason, the known measurements can only serve as comparative values. The covalent radius of hydrogen is given as R_1 = 31 pm [12] (instead of 53 pm).

Helium, with twice the atomic number (Z = 2), has a smaller radius. The measured value is: r_{He} = 28 pm.

To calculate the radius, all parameters of substantial influence are considered. The electric fields of the two protons in the nucleus act upon a shell electron in the

distance R_1, thereby reducing it, while the second shell electron on the opposite side of the nucleus, at a distance of $2R_1$, is attempting to stretch the radius. In the sum of fields, the field E_1 of a positive elementary charge occurs twice, reduced by the negative field under consideration of the doubled distance according to the proportionality 5.2 to the $(\frac{1}{2})^2$ (=0,25)-fold value. Normalized to E_1, the field resulting from the superposition is thus in effect:

$$f_2 = E_{ges}/E_1 = 2 - (\tfrac{1}{2})^2 = 1,75 \qquad (5.4)$$

The sum of fields is supposed to yield the atomic radius in the opposite direction:

$$\frac{R_{ges}}{R_1} = \sqrt{\frac{E_1}{E_{ges}}} = \frac{1}{\sqrt{f}} \quad \text{bzw.} \quad r_2 = \frac{1}{\sqrt{f_2}} = 0,756 \qquad (5.5)$$

Depending on how the radius of hydrogen was determined, helium's radius is decreased by a factor of 0.756.

$$R_{He} = 0,756 \cdot 31 \text{ pm} = 23 \text{ pm} \qquad (5.6)$$

resp. $\qquad R_{He} = 0,756 \cdot 53 \text{ pm} = 40 \text{ pm (classical)}$

The cited measured value lies in between, at 28 pm. The high uncertainty presumably is due to the immense difficulty in scanning the hydrogen cloud with precision. With increasing atomic number, uncertainty decreases, however, allowing for much more exact advance calculations.

At least, this simple example served to explain the calculation method of covalent radii.

5.5 Calculating the atomic radii of the 2s-orbital

With an atomic number of 3, lithium follows helium in the periodic system of elements. But the 1s-orbital, referred to as "K-shell" in the shell model, is fully occupied by two electrons enclosing the nucleus as hemispheres, already. The third electron has to occupy another shell, the L-shell or 2s-orbital, repeating the process described for the 1s-orbital.

The outer shell electron, on its way towards the nucleus, by which it is attracted, approaches the two 1s-electrons in the fully occupied K-shell, being repelled by which it expands (to approximately $R_o = 105$ pm). Once again, it's being deformed into a hemisphere whirling around the center as an electron cloud, which is why it's commonly referred to as an orbital.
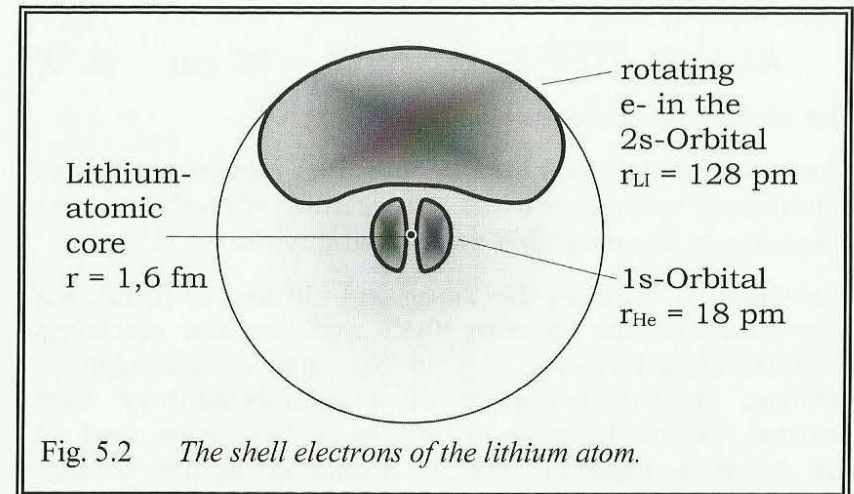
Fig. 5.2   *The shell electrons of the lithium atom.*

The 1s-orbital, after having formed a closed K-shell, is being further contracted depending on the atomatic number Z:

$$R_K = R_1 \cdot \sqrt{(1/Z)} \qquad (5.7)$$

$$= 31 \cdot \sqrt{(1/3)} = 18 \text{ pm} \qquad (5.8)$$

Together with the radius of the 2s-orbital of 105 pm, the radius of the lithium atom amounts to:

$$R_{Li} = 18 + 105 = 123 \text{ pm} \qquad (5.9)$$

This roughly corresponds to the measured value. I intend to refrain from further assumptions and postulates during the course of my calculation.

At Z = 4, the gap in the 2s-orbital is filled by another hemispherical electron, corresponding exactly with the structure of the inlying 1s-orbital.. According to the given rules, the radius of the beryllium atom thus calculates to:

$$R_{Be} = 31 \cdot \sqrt{(1/4)} + 105 \cdot 0{,}756 = 95 \text{ pm} \qquad (5.10)$$

The measured covalent radius is 96 pm.

The increasing agreement between measured and calculated values can be attributed directly to the precision of the available measurement values [12].

The electron cloud of the 2s-orbital alluded to in fig. 5.2 only concerns the exterior shell and singular electrons in particular, however, e.g. in the case of hydrogen or lithium. In the presence of a complementary spin partner, i.e. in the case of helium or beryllium, and all the more in case of heavier atoms of higher ordinal number, the electron clouds become ever more compressed, which is why the shell model with its K-, L-, M-, N-, O-, P-shells is being applied.

5.6 The 2p-orbital as an orange-model

The calculation of the beryllium atom's radius has shown the outer L-shell's (2s-orbital) radius to be about 5 times the size of the inner K-shell (1s-orbital). There remains room for up to six additional electrons. But as they're all striving towards the center where they are shrunk equally while expanding towards the exterior, they assume the shape of "peeled orange wedges". I therefore refer to the "orange-model" as a refinement of the shell-model.

In the orange-model, the electrons continue rotating around their own axes, despite distortion by the field of the nucleus and other neighboring electrons.

L-shell of Neon

R√2   R√2

Fig. 5.3. The orange as a model

They also form spin-complementary pairs and attract each other magnetically. The previously gathered insights hence remain valid.

In the case of carbon, an additional pair is present, making the peeled orange split into 4 even pieces when viewed from above. With respect to distance, one must substract the field of the neighboring electrons from the field of the Z -2 = 4 protons in the nucleus, whereby two electrons are at a distance of R·√2 and one at 2R. The scaling factor of the field is thus:

$$f_{Z-2} = f_4 = 4 - 2 \cdot (1/\sqrt{2})^2 - (\tfrac{1}{2})^2 = 2{,}75 \qquad (5.11)$$
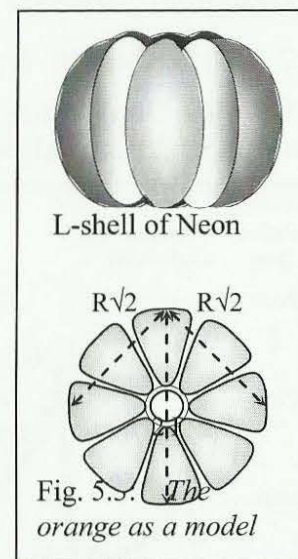
while the radius factor is: $r_4 = 1/\sqrt{f_4} = 0,6$. (5.12)

The radius of the carbon atom (for $Z = 6$) thus calculates to:

$$r_C = 31/\sqrt{Z} + 105/\sqrt{f_{Z-2}} = 75,97 \text{ pm} \qquad (5.13)$$

The measured radius is 76 pm.

Validating eq. 5.12 on the basis of boron:

$$Z = 5 \text{ (Bor): } f_{Z-2} = f_3 = 3 - 2 \cdot (1/1,62)^2 = 2,238 \qquad (5.14)$$

the measured and calculated values of 84 pm correspond perfectly. Further results are:

$$Z = 7 \text{ (Nutrition): } f_5 = 5 - 2,06 = 2,942 \qquad (5.15)$$

The measured value of 71 pm opposes the calculated radius of 73 pm. All values are listed in fig 5.4.
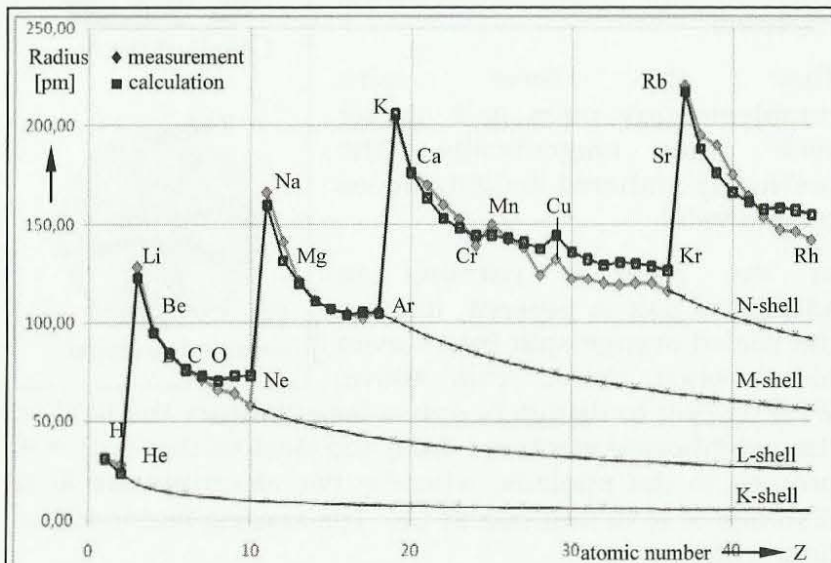
Fig. 5.4: *Atom radii calculated by sammation of the individual shells in comparison to measured values*

5.7 The radius calculation of all elements

The outstanding correspondence of calculated and measured values continues towards high atomic numbers, up until radon ($Z = 86$) and beyond fig. 5.5 shows the continuation of fig. 5.4.

The "sawtooth-like" measuring curve is known from literature [13]. The jumps around 105 pm reappear whenever an electron shell is occupied for the first time. Minor discrepancies between measurement and calculation occur in particular once lower shells are filled up with electrons. The calculation process presented here disregards these influences for now. The current collection of formulas is complicated enough.
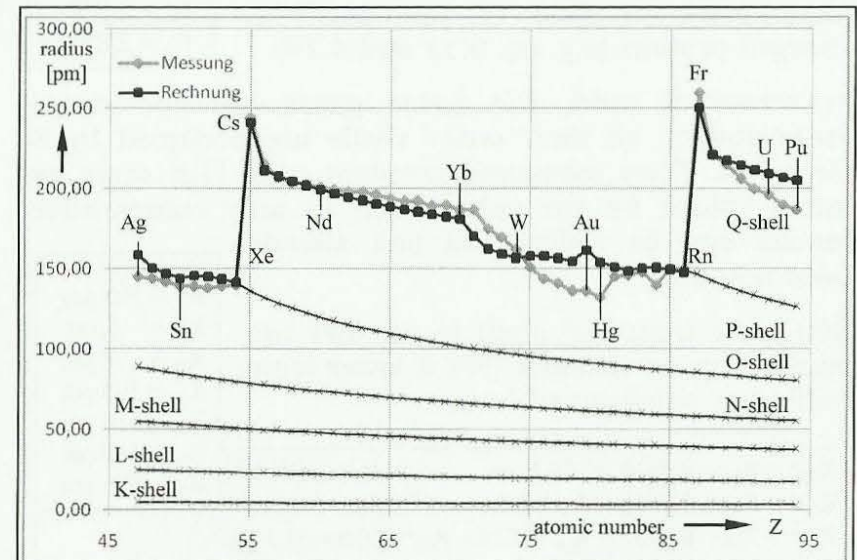
Fig. 5.5: Continuation of Fig. 5.4: *Calculated atom-radii in comparison to measured values.*

The radius of an atom of atomic number Z can be calculated by the formula:

$$R_Z = \frac{R_1}{\sqrt{Z}} + R_{10}*\sqrt{\frac{8}{Z-2}} + R_{18}*\sqrt{\frac{8}{Z-10}} + R_{36}*\sqrt{\frac{8}{Z-28}} +$$
$$+ R_{54}*\sqrt{\frac{8}{Z-46}} + R_{86}*\sqrt{\frac{8}{Z-78}} + \frac{R_o}{\sqrt{f}} \qquad (5.16)$$

In it, the field factors of the respective outer shell, containing between one and 10 electrons, are entered according to the accompanying table. As already explained, the factors are calculated by substracting the field of neighboring, negatively charged electrons with respect to their mutual distance from the uncompensated field of the positively charged protons (e.g. eq. 5.11 and 5.14).

$f_1 = 1$
$f_2 = 1,75$
$f_3 = 2,238$
$f_4 = 2,75$
$f_5 = 2,942$
$f_6 = 3,083$
$f_7 = 2,829$
$f_8 = 2,75$
$f_9 = 2,778$
$f_{10} = 2,87$

In terms of radii, the noble gases are considered authoritative, as their outer shells are occupied by 8 electrons. Their measured covalent radii [12] serve as initial values for the calculation, as only comparative results can be yielded, as has already been noted.

Distances from one shell to another are marked by an asterisk (R*) if lower-lying radii were substracted from it.

given radii:
$R_o = 105$ pm
$R_1 = 31$ pm
$R_{10} = 58$ pm
$R_{18} = 106$ pm
$R_{36} = 116$ pm
$R_{54} = 140$ pm
$R_{86} = 150$ pm

$R_{10}* = R_{10} - R_1/\sqrt{10} = 48,2$ pm   (5.17)
$R_{18}* = R_{18} - R_1/\sqrt{18} - R_{10}*\sqrt{8/16} = 64,6$ pm
$R_{36}* = R_{36} - R_1/\sqrt{36} - R_{10}*\sqrt{8/34} - R_{18}*\sqrt{8/26} = 51,5$ pm
$R_{54}* = R_{54} - R_1/\sqrt{54} - R_{10}*\sqrt{8/52} - R_{18}*\sqrt{8/44} - R_{36}*\sqrt{8/26} = 60,5$ pm
$R_{86}* = R_{86} - R_1/\sqrt{86} - R_{10}*\sqrt{8/84} - R_{18}*\sqrt{8/76} - R_{36}*\sqrt{8/58} - R_{54}*\sqrt{8/40}$
$= 64,2$ pm (K-shell) (L-shell) (M-shell) (N-shell) (O-shell)

For the precalculation of the radius of an atom of atomic number Z according to eq. 5.16, the element's main group, or which shells need or need not yet be considered, is also of relevance.

| |
|---|
| for the 1st cycle   Z = **1** to **2** are f = f_1, f_2 and the radii of the non existing shells: $R_{10}* = R_{18}* = R_{36}* = R_{54}* = R_{86}* = 0$ |
| for the 2nd cycle   Z = **3** to **10** are to be inserted as field factors f: f = f_1 to f_8 und $R_{10}* = R_{18}* = R_{36}* = R_{54}* = R_{86}* = 0$ |
| for the 3rd cycle   Z = **11** to **18** are f = f_1 to f_8 valid, at $R_{18}* = R_{36}* = R_{54}* = R_{86}* = 0$ |
| for the 4th cycle   Z = **19** to **28** are f = f_1 to f_{10} , and after that for Z = **29** to **36**:   f = f_3 to f_{10} ; $R_{36}* = R_{54}* = R_{86}* = 0$ |
| for the 5th cycle   Z = **37** to **46** are: f = f_1 to f_{10} , and after that for Z = **47** to **54** are: f = f_3 to f_{10} at $R_{54}* = R_{86}* = 0$ |
| for the 6th cycle   Z = **55**   is   f = f_1
 Z = **56** to **71** is   f = f_2
 Z = **72** to **78** is   f = f_4 to f_{10}
 Z = **79** to **86** is   f = f_3 to f_{10} ;   at $R_{86}* = 0$ |
| for the 7th cycle   Z = **87**   is   f = f_1 and for
 Z = **88** to **110** is   f = f_2 inserted.   (5.18) |

For example, it should be noted that all lanthanides (in the f-block) only have 2 electrons within their P-shell, merely filling up the lower N-shell from element to element. This lets the atoms shrink slowly. Of principal influence on the atomic radius however is the outer pair (for which f = f_2 applies).

The actinides behave in a similar fashion.

Despite formulating a rule applicable to all elements for the first time, the individuality of each and every element remains noticeable.

5.8 Calculation of ion radii

By consequent application of the calculation rules, ion radii can also be determined. The principal influence is once again the field factor f.

The elements strive for the configuration of a noble gas, for example neon ($_{10}$Ne), with its outer shell (L-shell) consisting of 8 orange wedges, as depicted in fig. 5.3. For this ideal arrangement, the field factor f_8 calculates to

$$
\begin{aligned}
f_8 &= 8 - 2\cdot(1/2\sin 22{,}5°)^2 - 2\cdot(1/\sqrt{2})^2 - 2\cdot(1/2\sin 67{,}5°)^2 - (\tfrac{1}{2})^2 \\
&= 8 - \quad 3{,}414 \qquad - 1 \qquad - 0{,}5858 \qquad - 0{,}25 \\
&= 2{,}75 \qquad\qquad\qquad\qquad\qquad\qquad\qquad\qquad (5.19)
\end{aligned}
$$

The field of the 8 protons responsible for the L-shell's contraction is thus reduced by the electrons which tend towards expansion due to their mutual repulsion. Their effect is reduced to approximately 5.25 because of the increased distances between one another. As before, the difference ($f_8 = 2.75$) determines the atomic radius of the noble gas neon.

If an additional electron is forced upon fluoride, or two upon oxygen, so that as negative ions their L-shells are fully occupied, they lack one or two protons, reducing the field factor to $f_7 = 1{,}75$ or $f_6 = 0{,}75$.

In case of the oxygen ion $_8$O^2, the calculated radius of 132.24 pm is very close to the measued radius of132 pm.

Elements normally possessing electrons within a higher shell display the opposite behavior: The partially filled outer shell is vacated and all its valance electrons removed.

The resulting ions now carry a positive charge. (e.g. $_{11}$Na$^+$, $_{12}$Mg^{2+}, $_{13}$Al^{3+}, $_{14}$Si^{4+}, etc.).

Taking the aluminium ion for example, the field factor thus increases by 3 to f = 5.75. The measured value is given as 57 pm [14], other sources claim 50 pm [15]. In any case, the calculation yields 52.38 pm.

Fig.5.6 provides the calculated ion radii and some measurement values.
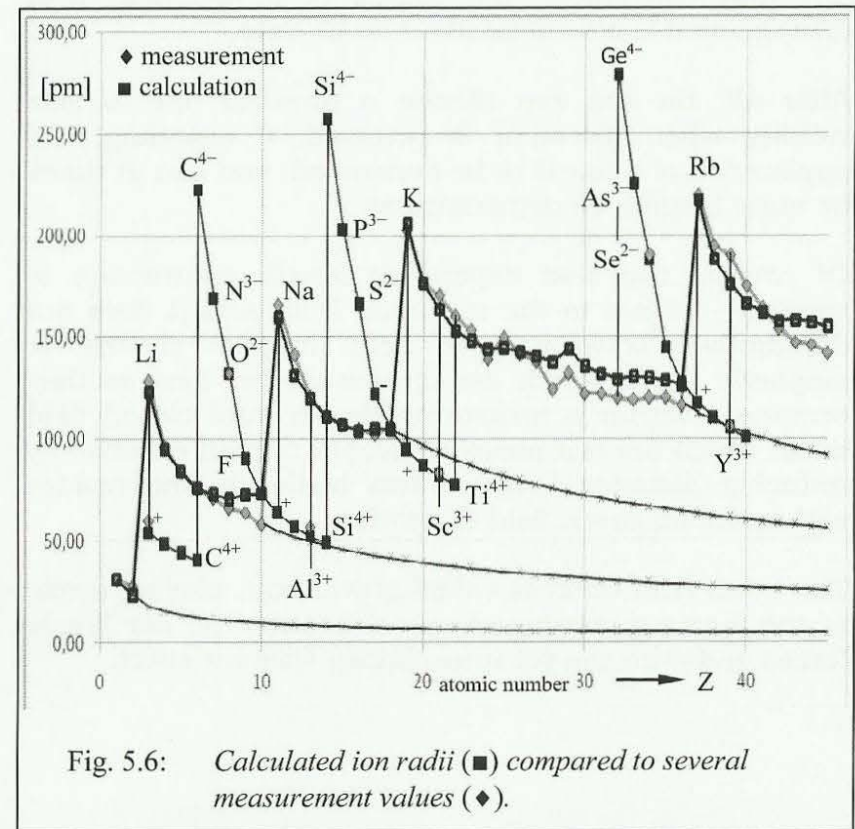
Fig. 5.6:   *Calculated ion radii (■) compared to several measurement values (♦).*

5.9 Summary of atomic radius calculation

The mathematical treatment of the topic and the conclusive comparison between measurements and calculations of atomic and ionic radii has clarified the "field dependent length contraction" considerably. This means that relativistically speaking, the electric field E, as externally observed, does not only diminish proportionally to distance squared (eq. 5.2: $E \sim 1/r^2$), but that conversely, the radius of a spherical field arrangement is also dependent on its field.

After all, no one can dictate a physical law to lose validity when direction is reversed. If anything, the application of a law is to be demanded, and can at times be quite helpful, as demonstrated.

Of course, the field dependent length contraction is similarly subject to the magnetic field. And it does not differentiate between open field lines of electric or magnetic fields, which are measurable as long as they terminate within a measuring device, and closed field lines, which are not measurable, yet remain effective by reducing distance between two bodies if one resides within the magnetic field of another.

The latter field effect is called gravitation, playing a role in the forces governing chemical bonds, Van der Waals forces and even the yet unexplained Casimir effect.

6. The vortex physics of chemistry

It is common practice in science to introduce new terms or postulates for phenomena discovered experimentally, yet lacking theoretical explanation. All too often, it is forgotten that this is but an intermediary solution.

One can quickly get used to such an illusory, parallel universe of physics and go on to presume one's own devised postulates to be authoritative. While inevitably turning out to be self-deception in the end, this can nonetheless be widely reflected in both general opinion and common text books.

Nowadays, anyone may lend his name to an observed force. There's not even a requirement to consult the known laws of physics for a possible explanation, first. For had that happened, we would have been spared the whole plethora of nuclear forces, atomic and chemical bonding forces, etc.

Which is why I am attempting to restore order to the arbitrariness of physical postulates, building upon the considerations of volume [2].

6.1 Ionic and atomic bonds

Let the foundation be the known and accepted "inverse square law" in its adequate interpretation, namely that all dimensions, measured in meters as per consensus, are determined (according to eq. 4.7) by the electric field E

$$E \sim 1/r^2 \qquad (6.1)$$

or in a similar fashion by the magnetic field H perpendicular to it

$$H \sim 1/r^2 \qquad (6.2)$$

by their given proportionality. In summary, one may speak of "the field", as the electric field is borne out of the magnetic field and vice versa, solely due to relative velocity. (Further pertinent information can be found in volume [1], transformation equations, or eq. 1.2).

The effects of the fields are manifold if a distinction is made between open and closed field lines, however.

Let's start with open electric field lines. They lead from a positive pole to a negative pole, e.g. from protons within a nucleus towards the electrons in the shell, where they terminate. If the amount of elementary charges in the nucleus is identical to those in the shell, the atom is electrically neutral as seen from the outside.

On its interior, however, the inverse square law applies (eq. 6.1). If the e^- is located within the field of the $p+$ or vice versa, both are reduced mutually, as well as their distance from one another, which is being interpreted as an attractive force.

It is the electromagnetic interaction, which ows its effect and range to the fact that its field lines converge towards the poles.

In case of equal polarity, the opposite occurs. The field lines repel one another and create a space in which the field approaches zero while distance approaches infinity, according to eq. 6.1. All these properties seem very familiar to us.

Which is why in chemistry, the forces of ionic bonding or polarized atomic bonding caused by the electromagnetic interaction are well understood Even electrically neutral molecules sometimes display a charge distribution within their near fields (partial charge according to electronegativity), which is subject to the electromagnetic interaction (also hydrogen bridges, for example).

Crystal lattices strive towards a structure of equilibrium between the attraction of negatively and positively charged ions and the simultaneous repulsion of equally charged ions or shell electrons. This results in a structure of minimal electric energy, or lowest energy level. To facilitate the mathematical handling, a corresponding energy level is designated to each ionization state.

In an atomic bond, the forces of the electric field are joined by the forces of the magnetic field, which stem from respective open field lines in an adequate manner. These have explained the cohesion of atoms and the pairing of shell electrons to us. The tendency to attain minimal volume and thus a low energy level is self-explanatory when considering electromagnetic forces.

6.2 Intermolecular forces

The question which forces hold nonpolar fluids together was of concern to Van der Waals. He did not understand them, yet gave them their name. Without them, no noble gas could ever be liquified. But it can. Liquid helium can thus be utilized as a coolant for supraconducting electromagnets.

If any forces exist, we can safely assume that they impact the microcosm as well. And so far, we have only considered half of the possibilities.

Besides open field lines, there exist those that are closed. Around every electric field line, a magnetic field line is wrapped in a closed vortex path and vice versa.. Both are perpendicular to one another. No one will doubt their existence, for they are founded upon the field equations of electromagnetism.

Fig. 6.1:   *The magnetic field is wrapped around the open electric field pointer in a closed vortex path and vice versa.*
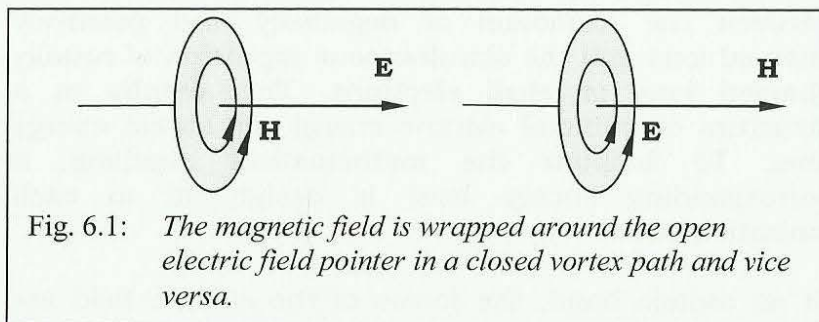
Curiously, no force interactions are ascribed to closed field lines at all, seemingly according to the mantra that "whatever is not measurable can not exist!". That is a capital mistake, however.

It is true that field strength can only be measured if a field line terminates in the measuring device, implying it must be open. In case of closed field lines, all methods of measurement fail, and yet they cause an effect nonetheless, which adheres to the proportionality of 6.1 or 6.2, respectvely. On the one hand, this inverse square law governs the diminishment of the (stray) fields with distance squared, on the other hand, it determines the magnitude of and distance between two field sources, as long as one resides within the stray field of the other.

In this case, no bundling of the fields occurs, consequently causing only very weak forces. In addition, they only exist as attractive and not as repulsive forces, as closed field lines are not supposed to cause interactions at all.

These ignored forces, present according to the law of physics, remain in effect even when not accompanied by open field lines.

As an example, consider an atom whose electric field lines all close internally within the shell, while externally, and theoretically to infinite distance, fields are emitted whose electric and magnetic field pointers orbit on closed vortex paths.

The effect of closed field vortexes is called gravitation (see derivation in vol. [2] ch.3). Its parameter is the unit of mass.

The inverse square causes the force to rapidly decline with distance. It should then show all the more explicitly up close. And in terms of intermolecular forces, this is clearly the case.

Naturally, the force increases for heavy nuclei, which manifests in the so-called intermolecular bond being significantly stronger in case of krypton and xenon than it is in case of the lighter noble gases helium and neon (dispersion force). More mass is equivalent to higher density of field lines.

Oftentimes, several forces are at work in superposition. This can complicate the determination of causes considerably (Debye force).

6.3 Casimir effect

If, in an experiment, two absolutely planar and smoothly polished metal plates are put in close proximity, an attractive force between them can be measured. Acting similarly to gravitation, but exceeding it significantly in magnitude, this has caused a lot of astonishment in scientific circles.
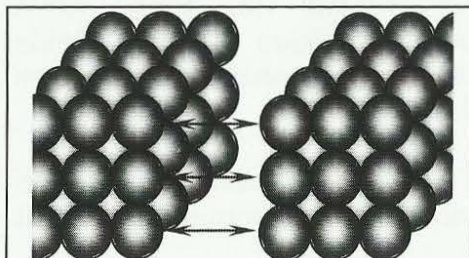
Fig. 6.2:   *The Casimir effect (attractive force between 2 plates).*

Close proximity means few atomic diameters here.
Today, we know that the Casimir effect persists in a vacuum and close to the absolute zero of temperature. Concurrent explanations range from zero-point energy to virtual or fluctuating particles.

Firstly, it is an adhesive force, the likes of which are utilized in various types of glue. In this regard, there are many parallels to the Van der Waals force. Therefore, there are forces at work that stem from closed field lines, specifically both electric and magnetic ones in tandem.

If the electrically conductive plates are moved together even closer, another effect emerges. While usually of an attractive nature, latest insights suggest reversibility. Judging by this property, it should be a superposition of open field lines.

If the plates are made up of a metal of odd atomic number, there are always open magnetic field lines which might be the cause.

Also, such substances display a high electrical conductivity if their valence band provides a singular uncompensated electron. This additional force would have to be considered in experiments wth e.g. gold-coated plates or spheres.

If both plates are made up of identical material, oscillations, as frequently occurring in the shell of metallic atoms, could play an additional role. Should the two opposing plates become resonant, an oscillating interaction would be the result, which would prove difficult to establish using concurrent measuring methods.

The simple example of the Casimir effect serves well to illustrate the complexity of all the possible interactions:

- Both open and closed field lines are a possibility,
- which might be either electric or magnetic,
- static or synchronously oscillating in resonance, all of which can create forces.

I count 23 = 8 combinations, which might occur either singularly or in any kind of superposition.

Any simplification, for example into electrostatic forces, eventually makes it necessary to widen the scope or introduce another force, postulate or name in substitution of a clear understanding.

Meanwhile, I demand nothing more than the strict observance and application of the inverse square law (1.3 or 6.1 and 6.2).

6.4 From plasma to fusion

Given sufficient energy influx, solid substances first transition into a liquid, then a gaseous, and finally a plasma phase. Usually, this goes along with an increase in temperature, with the temperature of the fourth state of aggregation depending on the ionizing energy of the respective substance. It determines the energy necessary to release one or more electrons from the atomic shell.

All over the world, scientists are working on so-called "hot fusion", in which the nuclei of light elements are to be fused in a plasma state. In this way, it is attempted to harness the released bond energy.

In order to prevent the electrons from interfering, in particular the ones closely enveloping the nucleus in the 1s-orbital, the nuclei are supposed to be laid bare, initially. According to the thinking outlined above, this would require extremely high temperatures. But the experiments don't go as the scientists had hoped, raising the possibility that errors in the model might be the cause.

The problems begin with the handling of the scorching plasma. Suspended within extremely strong magnetic fields, vortex currents emerge, which scatter the ions as expanding field vortexes (drop out effect through skin effect) instead of bringing them together.

The main problem, however, is the high temperature, an oscillation of magnitude as described in the derivation in volume [2] (ch. 6.3). Due to it, the partners never find one another. Even if a single fusion process should be observed by coincidence, it is hardly reproducible. At some point, we will realize that hot fusion is an aberration. The way to success will lead through cold fusion.

One again, nature is showing us the way. It employs another — let's call it the fifth — state of aggregation as a prerequisite for cold fusion.

7. Monoatomic nano-particles

Attaining new goals requires travelling on new and oftentimes unexplored paths, making science a highly interesting domain.

Have you ever heard about monoatoms, i.e. atoms that form neither molecular bonds nor crystal lattices? Can such white dust even be of interest? Biology agrees, while technology disagrees.

7.1 Literature on monoatomic elements

"If one divides metals into ever smaller pieces, they lose their metallic character", Scientific American proclaimed in 1989 [17]. There was talk about discovering a "new phase of matter".

The deformation of the nucleus during separation up to singular atoms is frequently described as oval [18, 19]. The proportion of diameter to height of the oval nucleus is supposed to be 1:2, as reported in Science News [20]. If the same article claims that isolated atoms rotate violently, it seems like a contradiction. The centrifugal forces occurring during rotation would suggest reversed proportions, i.e. a greater diameter and a lesser height.

A model for monoatoms is viable and scientifically valid only if it resolves such contradictions. And so the question remains why an atom of a precious metal would lose up to 41% of its weight once becoming monoatomic [21]. The experimental results pertaining to this weight reduction, established by David Hudson through analysis of larger amounts of monoatoms, may

be considered valid and reproducible; a true challenge for every scientist!

The numerous analyses have also elucidated which elements of the periodic system have been proven to occur in monoatomic form so far. With the exception of iron, they include all elements of the 8th subgroup (Co and Ni, Ru, Rh and Pd, Os, Ir and Pt). It includes all elements of the copper-group (1st subgroup with silver and gold), in addition to mercury and some rare earths (Lathanides Ce, Nd, Gd, Dy).

Noticeably, the metals from the 1st and 8th subgroup possess at least 6, 7, 8 or 9 electrons (in the d-orbital), which might be considered a prerequisite for the emergence of monoatoms. But carbon, nitrogen, oxygen and fluorine possess a similar amount of shell electrons.

If monoatoms exhibit a distinct state of aggregation, all kown elements should theoretically be able to attain it, even if it should prove stable for only few of them. All others would obviously regress into a known state on their own.

The question is: How does carbon, which is playing a key role, behave?

We know of carbon of three types: as graphite, as diamond and as fullerene (Bucky Ball). According to current knowledge, on Earth carbon mostly occurs as coal or graphite, with an abundance of more than 99.9%.

7.2 Atomic structure of carbon

Fig. 7.1:*The L-shell of carbon in the orange-model*
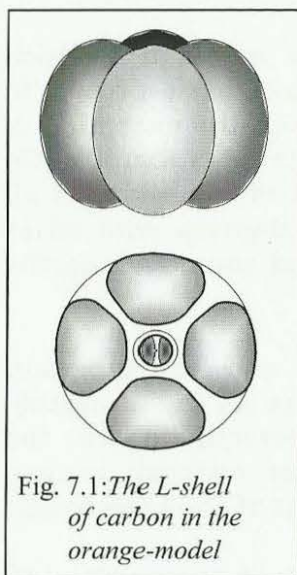
The nucleus consists of 6 protons and 6 neutrons (as shown in Fig. 3.9 on p. 35, nuclear radius: 2.22 fm).

Within the atomic shell, 2 of the 6 electrons are situated within the innermost K-shell, while the remaining 4 valence electrons are available for chemical bonding in the L-shell (atomic diameter: 76 pm, eq. 5.12).

The sectional view of a carbon atom depicted in Fig. 7.1 combines the experimentally gained knowledge about the orbital arrangement of the electrons with the vortex concept and the necessity of modifying the atomic model of Rutherford and Bohr, which is based on particles and therefore in contradiction to classical electrodynamics. On a centrally accelerated path, the electrons would have to emit energy perpetually before eventually crashing into the nucleus, which can not be observed at all. The existing, very small distances only permit the well ordered structure displayed.

Let's take a closer look at the possible structures of carbon, firstly graphite, secondly diamond, thirdly the Bucky Ball and lastly a fourth monoatomic structure, which remains largely unknown as of yet (possibly Carbon Black?).

7.3 Graphite and Diamond

In the case of graphite, the 4 valence electrons in the outer L-shell depicted in fig. 7.1 form pair bonds with neighboring carbon atoms. In this way, layers of carbon atoms are created which are stacked on top of one another. These layers form as every single carbon atom bonds with three neighboring carbon atoms, resulting in a hexagonal honeycomb pattern.

One electron within the L-shell remains free, it can move unimpededly along its plane and remains reactive. Ultimately, it determines the structure. In addition, these free electrons absorb light very effectively, explaining the jet-black color of coal.

Fig. 7.2:   *The layered honeycomb structure of graphite (left) compared to the diamond lattice (right)*
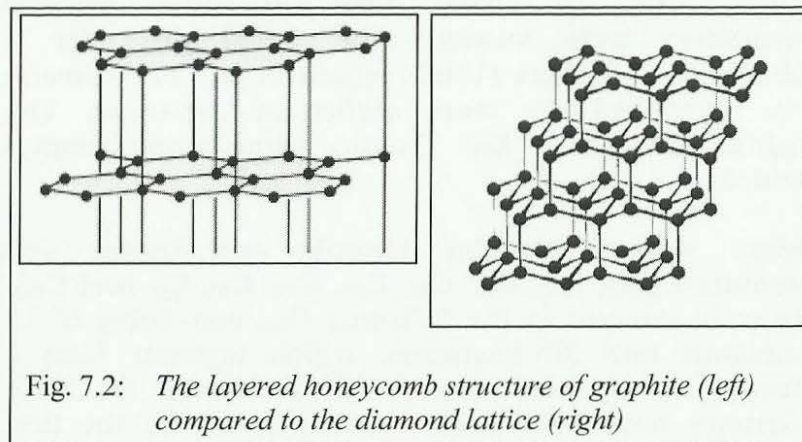
If, for example under high pressure, the layers come closer and the free electrons form bonds among the layers, an extraordinarily solid and now transparent network of carbon atom is formed, the diamond lattice (fig. 7.2). Due to our detailed knowledge of the lattice's

structure, it is nowadays possible to synthesize diamonds from graphite.

7.4 Fullerene, the 3rd structure of carbon

The third structure is reminiscent of a soccer ball sewn together from penta- and hexagonal pieces (fig. 7.3). If one were to use hexagonal pieces exclusively, the result would be a plane, i.e. graphite. The pentagons, however, bend the surface towards a sphere, the fullerene (Bucky Ball). In 1996, three researchers were awarded the Nobel prize for a publication in Nature (1985), which in fact had already been published 15 years earlier in Japanese. The original discoverer, Eiji Osawa, came away empty-handed.

Fig. 7.3: *The C-structure as fullerene*

Today, many molecular formula are known and researched (C_{60}, C_{70}, C_{76}, C_{80}, C_{82}, C_{84}, C_{86}, C_{90} and C_{94}). The most covered is the fullerene C_{60}, consisting of 12 pentagons and 20 hexagons, which together form a blunted icosahedron (soccer ball molecule). In 2010, fullerenes have been discovered in space for the first time. They are supposed to be the largest ever found molecules in space. C_{60} for example has a diameter of 0.7 nm.

On the basis of theoretical considerations and experimental findings, another yet disregarded fourth structure should exist: the monoatomic one.

7.5 Fabrication of the monoatomic structure

The monoatomic properties known from several metals make it impossible for singular atoms to enter lattice formations with other atoms, not even atoms of the same metal, due to their structure.
As such, they remain isolated and are perceived as indifferent and technically worthless dust. Accordingly, metrological results prove themselves difficult.

Multiple methods for artificial creation are known, with the following highly efficient mechanical method being especially elucidating regarding the structure of monoatomic elements. Once again, carbon will serve as example.

Fabrication is possible with so-called "defractoring machines". They utilize two counter-rotating impeller wheels with minimal distance and high rotational speed. If graphite powder is poured in between them, not only the crystal lattice is obliterated. Through shear forces, the carbon atoms are forced into quick rotation. Consequent to the high centrifugal forces, the accelerated shell electrons are heaved into a remote circular orbit. All electrons rotate around the exposed nucleus on a singular plane. This is comparable to the solar system, in which the central star is circled by its planets on the ecliptic plane.

Alternatively, the same result can be achieved by strong vortex acceleration. The necessary acceleration can for example be provided by a "Schauberger"-funnel tapering downwards, only assisted by gravity — passively, so to speak. Other methods rely on active whirlers driven by pumps.

If for example CO_2 is injected into such a water vortex, the molecule is split by the occurring centrifugal forces in the first stage. The oxygen is thereby released. In the second stage, the carbon atom is put into rotation and enters the monoatomic state in the third stage.

Practice shows that this state is not particularly stable, however. Especially in the presence of water, which absorbs rotational energy quickly, the monoatomic substance reverts back to conventional carbon, which now bonds with other atoms, forming chains and rings.

We know the resulting products as oil or gas. But should these substances turn out to be manufacturable, nature would be able to do so as well, meaning it would be justified to doubt conventional wisdom on the fossil origin of these products as well as their finiteness or regenerability.

7.6 The 4th structure of carbon

In this new structure, all shell electrons exhibit their elliptic particle structure and orbit the nucleus on a cicular path, steadily attracted by its positive charge. Thereby, their rotational axis shifts by 90°. so that the magnetic north pole of one electron is pointing towards the magnetic south pole of another. In this way, they form a more or less closed chain, which in the current case of carbon is not yet closed entirely, making sustained stability appear unlikely.

If the electric field pointer **E** is pointing outwards radially from the center and rotation is occurring with an orbit velocity **v** perpendicular to it, a magnetic field **B** is the result, which in turn is perpendicular to the plane formed by both **E** and **v** (according to eq. 1.2: **E** = **v** x **B**).

Fig. 7.4: *Monoatomic carbon with electron ring*
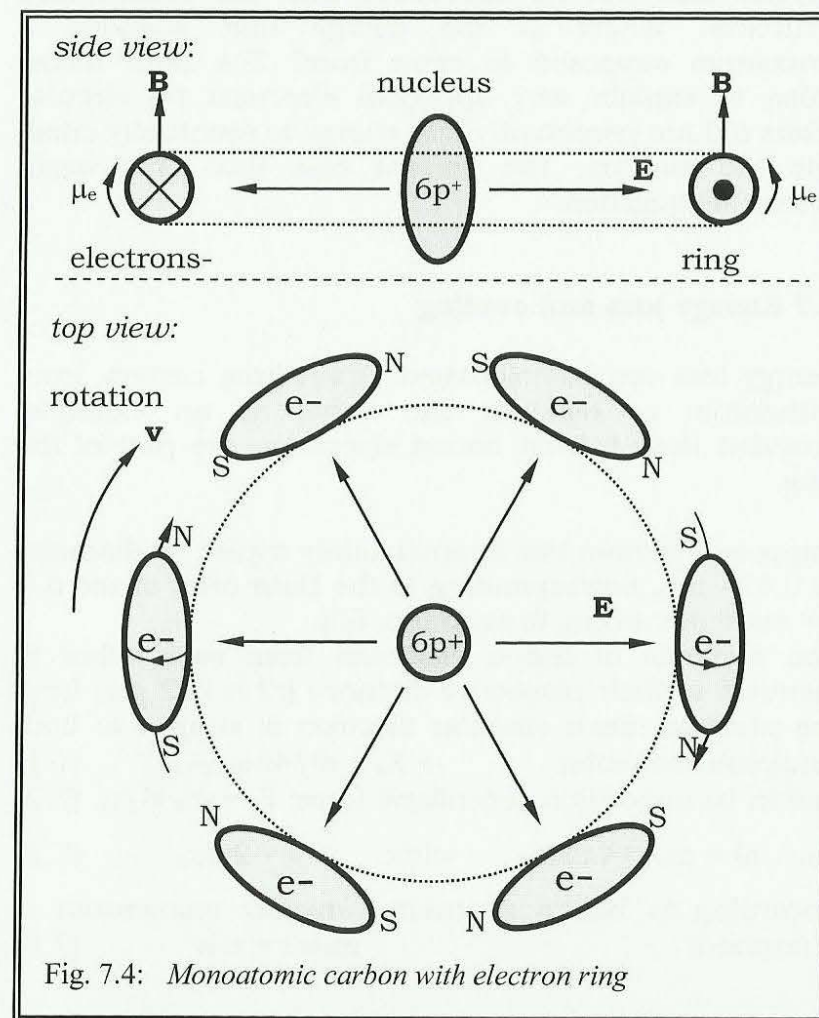
The high orbit velocity of the electrons prevents any lattice formation. Chemical reactions do not occur, which is why the field of chemistry has ignored this structure so far and has thus failed to recognize its true meaning.

Physics also has its difficulties with the monoatomic structure. Where is the energy that sustains a monoatom supposed to come from? The Bohr model failed to explain why spherical electrons on circular orbits did not perpetually lose energy to eventually crash into the nucleus. The present case thus once again poses this question.

7.7 Energy loss and cooling

Energy loss can be calculated. Apart from carbon, iron, ruthenium or osmium can serve as an example, provided their 6 least bound electrons are part of the ring.

Suppose the atom has approximately tripled its diameter to 0.424 nm, corresponding to the Bohr orbit of the n = 2nd state (according to eq. 5.3 p. 63).
The distance of the 6 electrons from each other is identical to their respective distance ($r2$ = 212 pm) from the nucleus. Each singular electron is subject to both Coulomb attraction $\quad -F_{el} = e^2/4\pi \cdot \varepsilon_o r_2^2 \quad$ (7.1)
and in its opposition centrifugal force: $F_z = m_e \cdot v^2/r_2$ (7.2)

so: $\quad e^2 = m_e \cdot v^2 \cdot 4\pi \cdot \varepsilon_o r_2 \quad$ with: $\quad v = 2\pi f \cdot r_2 \quad$ (7.3)

According to Bohr's postulate, angular momentum is quantized: $\qquad\qquad\qquad m_e \cdot v \cdot r = n \cdot \hbar \qquad$ (7.4)

The greater the radius r, the lesser the orbital velocity v and orbital frequency f, aiding in extending the interval until collapse of the monoatom and possibly promising longevity.

In the example, the orbital frequency calculates to:

$$f = e^2/8\pi^2 \cdot \varepsilon_o \cdot \hbar \cdot r \cdot n = 821 \cdot 10^{12} \,[\text{Hz}] \qquad (7.5)$$

This frequency is already above violet in the range of UV radiation.
Imagining the monoatom as an antenna, respective emissions in the direction of the magnetic field pointer due to the rotating electric charges are to be expected, which would occur continuously, as opposed to quantized in the case of normal atoms.

In practice, each monoatom will have a different diameter and therefore emit a different wavelength. This causes a blend of frequencies, which is called noise in terms of metrology.

On the one hand, the emissions of a rotating dipole are very weak, while on the other hand, they are easily drowned out by ambient noise. Observed for longer, the orbital radius will slowly decrease (from r_1 at v_1 to r_2 at v_2). The law of conservation of angular momentum applies, with the rotating mass being, as in eq. 7.2 : m = 6·m_e , i.e. the mass of all 6 shell electrons:

$$J \cdot \omega = m \cdot r^2 \cdot v/r = m \cdot r \cdot v = \text{const.} \qquad (7.6)$$

resp.: $\qquad m \cdot r_1 \cdot v_1 = m \cdot r_2 \cdot v_2 \qquad$ (7.7)

or: $\qquad v_2/v_1 = r_1/r_2 \qquad$ (7.8)

The conservation of angular momentum influences the energy balance, as: $E_{kin1} = (½) \cdot m \cdot v_1^2 \neq E_{kin2} = (½) \cdot m \cdot v_2^2$. Via conservation of energy, the difference calculates to:

$$\Delta E = E_{kin1} - E_{kin2} = (½) \cdot m \cdot (v_1^2 - v_2^2) \qquad (7.9)$$

$$= (½) \cdot m \cdot v_1^2 \cdot (1 - r_1^2/r_2^2) \qquad (7.10)$$

Therefore, if the electron ring became smaller over the time $(r_2 < r_1)$, the energy differential ΔE is negative; i.e. energy needs to be added externally. This important statement can be generalized:

> An imploding or contracting vortex cools its surroundings.

Much better known, however, is the reverse process, generally employed through explosion or expansion processes (combustion).

The influence on temperature, due to the change in volume under constant pressure according to Gay-Lussac, is calculated as an isobaric state change $(V \sim T)$. (Note: Because of energy or heat differentials, an adiabatic state change can be excluded, while the change in volume of $V = r^2 \cdot \pi \cdot h \sim r^2$ precludes an isochoric state change).

$$(T_1/T_2) = (V_1/V_2) = (r_1/r_2)^2 \qquad (7.11)$$

For $T_2 < T_1$ a cooling by the temperature differential ΔT occurs (valid for gases during isobaric state change if p = const.):

$$\Delta T = T_1 - T_2 = T_2 (r_1^2 - r_2^2)/r_2^2 \quad [K] , \qquad (7.12)$$

which is why a contracting vortex usually withdraws radiation heat from its environment.

8. Nano-technology

To egalize the energy balance, monoatoms on Earth have a wide spectrum at their disposal, from infrared light to visible light up into the ultraviolet, the range that permeates the ionosphere. Conversely, the absorption of radiation demands an according dimensioning of the ring antenna, allowing conclusions to be drawn about the monoatom's size. Presumably, these reach far into the nanometer range, preferably on the orbits provided by Bohr (for n = 2, 3, 4, 5, 6, 7).

In summary, the following picture emerges: unstable monoatoms shrink over time while increasing frequency. Meanwhile, acting as a ring antenna, they emit a blend of frequencies as antenna noise in the direction of the magnetic field pointer, compensating their energy demands by drawing power from their surroundings.

When it comes to nano-technology, observing a decrease in temperature therefore is a clear indication of the nano-particles being monoatoms during the shrinking process.

Conversely, processes to manufacture nano-particles from gaseous raw materials are known which generate small solid particles by condensation through rapid cooling [22].

The occasionally observable weight loss and the oval shape of the nucleus remain unsolved and irreconcilable with classical physics, however.

8.1 The ellipsoid nucleus

The same calculation rules shall be applied that were used to succcessfully determine the quantum properties of elementary particles mathematically. Once again, a fundamental building block is the field dependent length contraction.

$$(6.1: r^2 \sim 1/\mathbf{E} \quad \text{and} \quad 6.2: r^2 \sim 1/\mathbf{H}).$$

The calculation of the mass of an elementary particle as well as that of the entire nucleus is performed by analysing the involved field lines and thus ultimately the mutual influence exerted by a particle on its neighbors and vice versa, which shrinks them in the process.

When an atom turns into a monoatom by rearranging its 6 to 8 valence electrons into a ring, the nucleus' charge and consequently field lines remain unchanged. Only the direction of the electric field lines changes. They no longer point in all directions, as with the sphere, but instead all point into the ring (fig. 7.4), which is a novelty.

Conversely, all field lines stemming from the ring electrons now point towards the nucleus' "equator" rather than its "poles". Yet if the field at the equator increases, the nucleus's radius is reduced, while a simultaneous decrease of the field at both poles increases the polar radius. The result is an elongated sphere, a so-called ellipsoid.

This result contradicts our experience, which says that nuclei tend towards a spherical shape, as it guarantees the gihest possible packing density. The threshold of stability is reached with uranium, of atomic number 92. If however the nucleus is deformed, as is the case with monoatoms and their elongated nuclei, this threshold should logically be crossed much earlier.

According to current knowledge, gold and mercury (of atomic numbers 79 and 80) are the largest still stable nuclei in nano-structures. The atomically stable lead could however not yet be found or produced in monoatomic form. Still, its principal instability makes it suitable as raw material and energy supplier for the production process of the nano-particles.

8.2 The mass reduced nucleus

Why are microcosmic particles the heavier the smaller they are? Textbooks don't hold the answer for the most central of questions in quantum physics.

Looking at the particles from outside, i.e. through our eyes or suitably designed microscopes, Newtonian mechanics, the laws of optics and the theory of relativity aid us in determining their quantum properties. For this case, volume[3] (with eq. 3.35 in the so-called observation range) derived the proportionality for the determination of particle mass:

$$m \sim 1/r \qquad (8.1)$$

As the mass is mostly confined to the nucleus, the electrons orbiting in the ring have only a negligible influence on the total mass and the ring diameter only plays a minor role.

During the formation of the monoatom, the calculated energy excess does arise, however, and is partially absorbed by the nucleus through increased rotation.. The measured weight reduction to 5/9th that of the original metal [23] suggests that the nucleus has been elongated by 80% through centrifugal forces.

$$m_2/m_1 = 5/9 = r_1/r_2 \quad \text{and} \quad r_2 = (9/5)r_1 = 1{,}8r_1 \quad (8.2)$$

The ratio of the elliptically deformed nucleus' height over width would thus be 1,8:1. According to Science News, a ratio of approximately 2:1 has been measured [20]. Considering measurement uncertainties, this result bears the characteristic of proof.

In the face of vortex physics' superiority, the failure of quantum physics needs not be emphasized.

8.3 Monoatomic hydrogen gas (so-called Brownsgas)

Another possible way of producing monoatomic oxygen is noteworthy. It involves high voltage electrolysis. Through it, water molecules with their dipole nature are ripped apart under high electric field strengths and their components subsequently set into rotation.

The thusly created hydrogen gas (also referred to as Brown's gas) is hardly reactive and can be funneled safely to a welding torch through a single pipe. This is far from normal, as hydrogen and oxygen are usually led through separate pipes for safety reasons.
In the case of the monoatomic gas, however, the atoms rotate along without taking much notice of their surroundings. The welding torch's flame is unusually cold, luring the brave into holding their fingers right into the open flame. A thermal camera indicates less than 250°C.

If this flame is brought into contact with basalt or glass, however, it will melt at temperatures in excess of 1200°C. In this way, I could permanently fuse fibre optic cables of various qualities at an institute of Prague University, which had hitherto been impossible with conventional tools.

I believe the reason for this high melting temperature lies in the release of the rotational energy when the monoatomic flame comes into contact with the glass sample. Furthermore, I presume that the rotating monoatoms influence the structure of the valence electrons of the silicium dioxide sample.

8.4 Nano-molecules

SiO_2 has a special property, which it shares with CO_2, GeO_2 SnO_2 as well as TiO_2t. It is suitable as a monoatomic molecule if every oxygen atom supplies four electrons for the ring, specifically.the four electrons not involved in bonding. This enables the formation of the aforementioned 8-ring.

Through trial-and-error, nano-technology has long understood this and learnt to reap its benefits in industrial care and impregnation products.

Fig. 8.1: *monoatomic carbon dioxide*
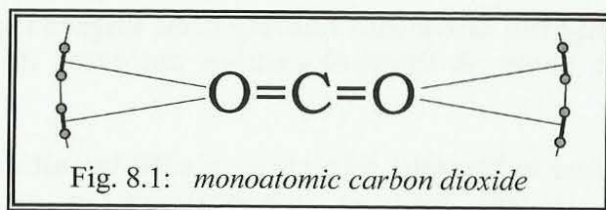
Plants also need these substances. The CO_2 required for photosynthesis is but one example. Increasing the concentration of carbon dioxide does not lead to an immediate increase in growth.

Only at nano scales, in a monoatomically swirled structure, the increase of approximately 100% is no longer non-obvious. For this reason, industrial CO_2 is swirled into water by the method outlined, and the plant then hydrated with it. The biological effect of the nano-particles is undisputed.

In this volume, the emphasis is on technical and physical properties, for example the question why 8 ring electrons are optimal. The answer can be found in fig. 7.4, depicting the 6-ring of carbon (possibly Carbon Black).

As shown, the electric fields not only deform the nucleus into an ellipsoid, but also the electrons in the ring on the other end of the field lines As one can see, there remains room in between the six electrons. If they are increased to eight, they have contact and the ring is closed (fig. 8.2).

This works because the electrically repellant particles are attracted magnetically, for each points its north pole towards its neighbors south pole, amplifying the effect the closer they get.

Fig. 8.2: Eightfold ionized molecule with *electron ring*
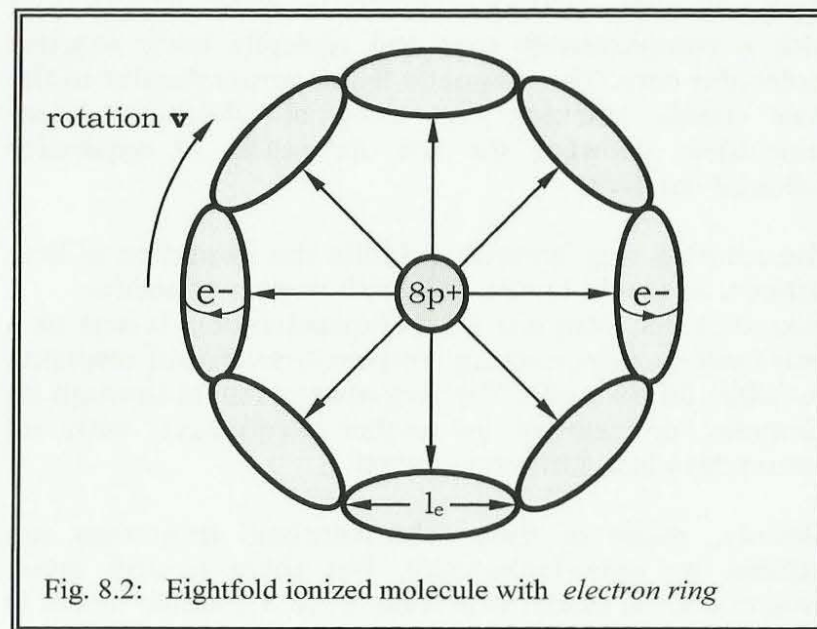
A magnetically closed ring could of course consist of an arbitrary number of electrons, but the distance to the positively charged nucleus would vary, with distance to similarly charged neighbors remaining constant. Stability could not be maintained in this way.

Which is why most nano-molecules are characterized by their 8 ring electrons. In the case of zinc oxide ZnO, zinc 2 and oxygen provide the remaining 6 electrons. Identical conditions are found in the semiconductors cadmium telluride (CdTe) and cadmium selenide (CdSe). Meanwhile, the closed electron orbitals situated in and around the nuclei are highly concentrated in their positively ionized structure.

Nano-molecules are shaped like a disk, circular and with a comparatively tiny and typically lowly reactive molecular core. The magnetic fields perpendicular to the disk enable stacking and tiling of additional nano-molecules, allowing for the formation of expansive colloidal clusters.

The rotating ring however inhibits the formation of firm lattices, as would be the case with metals or solids.
Also, it is free from any kind of quantization. It acts as a universal storage, making temperature-neutral reactions possible, for example. The ring always reacts through its diameter or velocity (or rather frequency), with all parameters being interconnected.

Already, many of these characteristic properties are utilized by nano-technology, but there is still much progress to be made, especially once a feasible model is established.

As for high voltage electrolysis, the combination of energy input and increase of reactivity opens up entirely new and exceptional possibilities in regards to the welding test.

Even cold Browns gas, entirely without being combusted, was supposedly observed to cause substance transformations, so-called transmutations, as well as alter radioactive half-lives. Are such speculations to be taken seriously from a scientific point of view?

8.5 Cold fusion

Monoatomic carbon depicted in fig. 7.4 and oxygen with all of its electrons in the ring, as shown in fig. 8.2, have one thing in common:

The nucleus is exposed!

This is a mandatory precondition for fusion. Contrary to hot plasma, in this case the nucleus is cold, however. Therefore, there exists no risk of repulsion through thermal movements or pulsations.

This reminds me of the hydrogen bomb, which cools the fusion process down to absolute zero via implosion (according to eq. 7.9).
Here, under supraconducting conditions, ideal circumstances for fusion are achieved, as nature only knows of cold fusion. Hot fusion, as a mere doctrine, lacks all scientific basis.

In the absence of technical solutions, nature is once again the prime example for the successful utilization of cold fusion. Take the "sodium-potassium-pump", which moves ionized molecules in opposition to the electric resting potential of a cell membrane as well as the predominant concentration gradient. After all, the concentration of K+ within a cell is more than 100 times that of Na+ on the opposite side of the membrane. How is this supposed to work?

Suppose a sodium ion ($_{11}^{23}$Na+) comes into contact with monoatomic oxygen ($_8^{16}$O): the nuclei, mutually attracted through magnetism, will fuse into a potassium ion ($_{19}^{39}$K+). The 8 ring electrons of the oxygen will be

decelerated in the process and form a new M-shell around the already occupied L-shell of the Na+..

Of course, there is more to the whole picture. This is merely an attempt to describe the basic process in order to provide a physical explanation free from contradictions. How the body supplies the oxygen and energy required, as well as the role played by ATP (adenosine triphosphate) are another story altogether.

If nature has mastered the use of monoatomic oxygen, then why wouldn't fusion involving carbon along similar lines also be a possibility? Regarding this case, a highly conclusive example is known: The experiment with the "dumb" chickens, who exhibit astonishing capabilites besides their capacity to lay eggs [24].

The animals were given chicken feed that was mostly deprived of calcium. The chickens however didn't seem to care and continued diligently laying eggs. The experimenters began to wonder what the lime source required for the egg shells might be. How does a chicken overcome this resource deficiency?

Further on, additional substances were removed from the the feed, and lo and behold, once silicium was withdrawn, the laying of eggs ceased. The inevitable conclusion of this experiment seems to be that chickens are somehow able to perform cold fusion, turning silicium $(_{14}^{28}Si)$ into calcium $(_{20}^{40}Ca)$ on demand, presumably with the assistance of carbon $(_{6}^{12}C)$.

The fusion process leaves the chicken cold, i.e. as with the Na+-K+-fusion pump, the process is neither exo- nor endothermic. The (negative) energy stored within the ring obviously brings about the necessary balance.

This is in stark contrast to technical attempts to harness fusion energy. They are supposed to generate heat in order to drive steam turbines, as power plant operators are quite capable in this regard.

The desired end product of fusion is usually a noble gas. The publically financed efforts are concerned with the fusion of deuterium into helium, a conventionally feasible process promising a high energy yield.

8.6 Transmutation

Unconventional processes are those involving monoatomic structures and remain largely ignored as of yet. They offer various avenues, for example the highly speculative "combustion" of water. Ideally, it could split heavy water D_2O into its base components through the aforementioned high voltage electrolysis or mechanically via defractoring, whereby the 8 shell electrons of the oxygen would from the ring.

The highly reactive monoatomic oxygen is suitable for many purposes. It could, with a high energy yield, fuse with two deuterium nuclei into neon, or alternativey into argon with another oxygen nucleus.

Genereally speaking, it can transform elements of the 2nd group into the corresponding elements of the 3rd group, or some of the elements of the 3rd group into those of the 4th (as discussed in regards to the sodium-potassium-pump).

However, the energy balance of this process is oftentimes negative. This method is therefore better suited for transmutation, a targeted substance transformation.

New transmutation products can also be observed in reactions involving monoatomic oxygen and heavy nuclei (such as tin or lead). Frequently, they are monoatomic themselves, with the energy balance being decisive.

Whoever is fascinated by the created substances, particularly the gold, which on this world supposedly exists much more abundantly as monoatomic white dust rather than golden glistening metal, will soon realize that little is known about rematerialization.

Practical experience regarding the extraction of the dust through magnetic latches is available, however.
After all, monoatomic elements only interact through their magnetic field. In accordance to the model presented (fig. 7.4 and 8.2), this technology appears both plausible and feasible.

If, the ring electrons shall also be captured and integrated into their designated shells, it results in cooling. It is said that supplying the energy required via UV light holds promise.

Experiments involving monoatomic carbon should prove themselves to be equally promising. They would pave the way for fusion into magnesium and even further into the noble gas argon:

$$(_6{}^{12}C + _6{}^{12}C \rightarrow _{12}{}^{24}Mg \quad resp.. \quad _{12}{}^{24}Mg + _6{}^{12}C \rightarrow _{18}{}^{36}Ar)$$
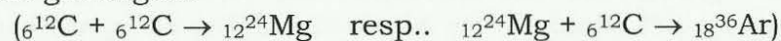
or the fusion of an alkali metal into a halogen:

$$(_3{}^7Li + _6{}^{12}C \rightarrow _9{}^{19}F \quad resp.. \quad _{11}{}^{23}Na + _6{}^{12}C \rightarrow _{17}{}^{35}Cl)$$
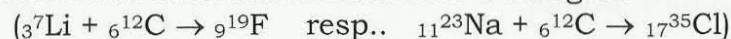
8.7 The 5th state of aggregation

The four known states of aggregation are solid, liquid, gaseous and plasma. With their special properties, monoatoms obviously represent another distinct state of aggregation, with close similarities to gases, for both do not form lattices.

Without chemical bonds, disk-shaped, and forming a ring with a positively charged nucleus, it fulfills all the conditions that Bohr's model for n =1 could not.

If the obsolete model is consulted in regards to the state sought by mono-atomic elements (for n = 2, 3, ...) and the amount of electrons required for an ideal ring, however, a lot is explained (line spectra, Rydberg formula, etc.).

n	Z_e	nuclear radius	frequency
1	2	$r_1 = 53$ pm	$f_1 = 6{,}58 \cdot 10^{15}$ Hz
2	8	$r_2 = 212$ pm	$f_2 = 821 \cdot 10^{12}$ Hz
3	18	$r_3 = 477$ pm	$f_3 = 243 \cdot 10^{12}$ Hz
4	32	$r_4 = 848$ pm	$f_4 = 103 \cdot 10^{12}$ Hz
5	50	$r_5 = 1{,}3$ nm	$f_5 = 53 \cdot 10^{12}$ Hz
6	72	$r_6 = 1{,}9$ nm	$f_6 = 30 \cdot 10^{12}$ Hz
7	98	$r_7 = 2.6$ nm	$f_7 = 19 \cdot 10^{12}$ Hz

The circumference of the ring is:

$$2\pi r = Z_e \cdot l_e \qquad (8.3)$$

at a length of e⁻ of

$$l_e = 166{,}5 \text{ pm} \qquad (8.4)$$

(see fig. 8.2)

Thus, light is created during the transition from n=3 to n=2, for example, as the interval from f_3 to f_2 contains all frequencies of the visible spectrum. In case of the even larger nano-particles, heat is generated in the form of IR radiation in the range off$_3$ to f_7.

In numerous chemical reactions, this 5th state of aggregation occurs during a short-lived transition phase, just before the valence electrons have rearranged and settled into their final configuration.

Is this the rebirth of Bohr's model? Generations of students have been wondering what is supposed to be wrong with it; why the radii for $n \neq 1$ were invalid, given that the wrong radii yielded the right line spectra and a fluorescent light shone nonetheless. "It is the noble gas' 8 valence electrons, electrically excited and heaved into a ring, descending back from the 3rd into the 2nd orbit." would be an answer free from contradiction.

What gases can do, solids can, too. If they are in a monoatomic state, we can only perceive fine dust instead of solid gold or liquid mercury, which by the way supposedly is no longer toxic when monoatomic due to the loss of reactivity [23].

The alchemists of ages past have become the nano-technicians of today. Thanks to outstanding microscopes, they can irectly observe monoatomic elements and witness their transformations. They are also the first to be able to marvel at the fantastic properties of nano-particles.
And so, there is still hope that one day, we will be able to make dusty gold shine...

oOo·oOo·oOo·oOo·oOo·oOo·oOo·oOo·oOo·oOo·oOo·oOo·oOo·oOo

9. Table of formula symbols

Electric field			Magnetic field		
E	V/m	electric field strength	H	A/m	magnetic field str.
D	As/m^2	electric displacement	B	Vs/m^2	flux density
ε	As/Vm	dielectricity	μ	Vs/Am	permeability
Q	As	charge	ϕ	Vs	magnetic flux
e	As	elementary charge	m	kg	mass
τ_2	s	relaxation time constant of the potential-vortices	τ_1	s	relaxation time constant of the eddy currents
			$\tau_1 = \varepsilon/\sigma$		

other symbols and definitions:

specific electric conductivity		σ	Vm/A
speed		v	m/s
speed of light	$c = 1/\sqrt{\varepsilon \cdot \mu}$	$= 2,9979 \cdot 10^8$	m/s
dielectricity	$\varepsilon_o = \varepsilon/\varepsilon_r$	$= 8,8542 \cdot 10^{-12}$	As/Vm
permeability	$\mu_o = \mu/\mu_r$	$= 4\pi \cdot 10^{-7}$	Vs/Am
angular momentum	$\hbar = h/2\pi$	$= 1,0546 \cdot 10^{-34}$	Nms
nucleus magneton:	$\mu_N = e\hbar/2m_p$	$= 5,0508 \cdot 10^{-27}$	J/T)
Bohr's magneton:	$\mu_B = e\hbar/2m_e$	$= 9,274 \cdot 10^{-24}$	J/T)
mass of electron	m_e	$= 9,1094 \cdot 10^{-31}$	kg
classical electron radius	r_e	$= 2,8179 \cdot 10^{-15}$	m

number of involved elementary vortices	z_e	-
rotational angular of nuclear particles	ξ	-

Landé-factor	g		nm	$= 10^{-9}$	m
atomic number	Z		pm	$= 10^{-12}$	m
number of neutrons	N		fm	$= 10^{-15}$	m
mass number	$A = Z + N$		$_z^A$element^{charge}		
proton	p^+		spin	s	Nms
electron	e^-		force	F	N
elektron neutrino	ν_e		radius	R,r	m

10. Bibliography

1:    Meyl, K.: Potentialwirbel Band 1, Über Wirbelphysik zur Weltgleichung, *INDEL* Verlag Villingen-Schwenningen, 2. Auflage 2012

2:    Meyl, K.: Potentialwirbel Band 2, Über Objektivität zur Einheitlichen Theorie, *INDEL* Verlag Villingen-Schwenningen, 2. Auflage 2012

3:    Meyl, K.: Potentialwirbel Band 3, Über Feldwirbel zur Physik der Elementarteilchen, *INDEL* Verlag Villingen-Schwenningen, 2. Auflage 2012

4:    Kaiser, D. (pseudonym): Kernphysik nach der Meyl'schen Feldtheorie, Manuskript, Knittlingen 2009.

5:    www.Wbabin.net/files/4597_yue1.pdf

6:    Bericht über experimentell gefundene Formen von Atomkernen am Kernforschungszentrum Karlsruhe, Bild der Wissenschaft, Heft 1, 1974, S.44.

7:    Bauer, W.: Die Welt der Wirbel und Atome, Skripten-Sammlung, Graphia Druck Salzburg 1975

8:    Stierstadt, Klaus: Physik der Materie, VCH 1989, S.87

9:    Schneller als Lichtgeschwindigkeit, Neutrinos laut CERN immer wahrscheinlicher, Focus Online vom 18.11.2011 und R. Vaas: Schneller als Einstein erlaubt? Bild der Wissenschaft, 11/2011, S. 52-55

10:    C. S. Wu, E. Ambler, R. W. Hayward, D. D. Hoppes, R. P. Hudson: Experimental Test of Parity Conservation in Beta Decay. In: Physical Review. 105, 1957, S. 1413-1415. doi:10.1103/PhysRev.105.1413

11:    Dr. Tesla writes of various phases of his discovery, New York Times, Feb.6, 1932, P.16, col.8.

Kovalenzradien für Atome in Einfachbindungen:
12:    Pekka Pyykkö, Michiko Atsumi: Molecular Single-Bond Covalent Radii for Elements 1–118. Chemistry - A European Journal, 2008, DOI 10.1002/chem.200800987.

13:    Lautenschläger, Schröter, Wanninger: Taschenbuch der Chemie. 20.Aufl. Verlag Harry Deutsch, 2007, S.108.

14:    www.chemie-master.de. Arbeitsblatt „Atomradius und Periodensystem der Elemente", Stand 03.02.2012

15:    Huttner: Grundvorlesung, Kapitel 2.7 Atom- und Ionen-Radien, S.8, Universität Heidelberg, 2011.

16:    Quanteneffekte bei Nanostrukturen, Spektrum der Wissenschaft, September 2009, S. 12; Interplay between geometry and temperature for inclined Casimir platesabstract@nasa ads; Physical Review D, vol. 80, Issue 6, id. 065033

17:    M.A.Duncan, D.H.Rouvray: Microclusters, Scientific American Dec.1989, p. 110 - 115.

18:    Physics Today, Vol.41, Nr.2, S.17

19:    Science News, Vol.133, S.347

20:    Steffi Weisburd: Superdeformed Nuclei go for a Spin, Science News, Vol.133, May 28, 1988, p.346f.

21:    David Hudson: brit. Patent Nr.: GB 2219995 A, Date of A publ. 28.12.1989

22:    F.Schmidt: Aufwändige Alleskönner – Nanoteilchen, Wissen&Umwelt, DW.De, Meldung vom 20.01.2012

23:    David Hudson: White Powder Gold – A Miracle of Modern Alchemy, Nexus Magazine, Vol.3, Nr.5 und 6, Aug./Sept. und Okt./Nov. 1996, und Science of the Spirit Foundation, Newsletter No.6&7, März/April 1996

24:    Louis Kervran: Biological Transmutations, s.a. J. Heinzerling: Energie aus dem Nichts, Bettendorf'sche Verlagsanstalt, 1. Aufl. 1996, S.278